RI 7901

Bureau of Mines Report of Investigations/1974

Blast-Produced Fractures in Lithonia Granite

UNITED STATES DEPARTMENT OF THE INTERIOR

Report of Investigations 7901

Blast-Produced Fractures in Lithonia Granite

By David E. Siskind and Robert R. Fumanti
Twin Cities Mining Research Center, Minneapolis, Minn.

UNITED STATES DEPARTMENT OF THE INTERIOR
Rogers C. B. Morton, Secretary

BUREAU OF MINES
Thomas V. Falkie, Director

This publication has been cataloged as follows:

Siskind, David E

Blast-produced fractures in Lithonia granite, by David E. Siskind and Robert R. Fumanti. [Washington] U.S. Bureau of Mines [1974]

38 p. illus., tables. (U.S. Bureau of Mines. Report of investigations 7901)

Includes bibliography.

1. Granite—Georgia. 2. Granite—Blast effect. I. U.S. Bureau of Mines. II. Fumanti, Robert R., jt. auth. III. Title. IV. Title: Lithonia granite. (Series)

TN23.U7 no. 7901 622.06173

U.S. Dept. of the Int. Library

CONTENTS

ILLUSTRATIONS

ILLUSTRATIONS--Continued

TABLES

BLAST-PRODUCED FRACTURES IN LITHONIA GRANITE

by

David E. Siskind[1] and Robert R. Fumanti[2]

ABSTRACT

The Bureau of Mines has studied the fracturing produced in the vicinity of large-diameter blastholes in Lithonia granite. Cores were taken from the vicinity of AN-FO production blasts and examined using a total of seven laboratory and field measurement techniques to delineate zones of damage and evaluate the effectiveness of the seven diagnostic tests for fracture-state determination.

Laboratory measurements of acoustic pulse velocity, porosity, permeability, compressive strength, and Young's modulus indicated the extent of fracturing with the acoustic techniques providing the best means of distinguishing between fractured and unfractured core.

A severely fractured zone was found to extend approximately 25 inches (64 cm) from the center of the 6-1/2-inch blastholes, equivalent to 8 blasthole radii. A second zone, characterized by a lesser degree of fracturing extended from 25 to 45 inches (64 to 114 cm) or 8- to 14-blasthole radii. Beyond 45 inches (114 cm) the rock was undamaged.

INTRODUCTION

This Bureau of Mines report discusses the analysis of fracture damage produced around large-diameter (6-1/2-inch) blastholes in Lithonia granite, Lithonia, Ga.

Explosives are extensively used to fracture rock for mining and excavation. A quantitative understanding of the fracturing and crushing that occur in a blast vicinity is necessary in an attempt to control excavation limits and prevent overbreak. In underground mining, rock competency must be maintained outside the desired volume of excavation in order to reduce blasting damage contributing to subsequent roof failure. Examples of controlled blast-produced fracturing are presplitting, the use of decoupled light charges in the perimeter holes of tunnel excavations and mine drifts for smooth blasting,

[1]Geophysicist.
[2]Engineering technician.

and fracturing for in situ mining. In situ mining provides many advantages over conventional surface and underground mining and will see increased application in the future. Here, explosives are used to fracture a rock mass for passage of leaching or retorting solutions (metallic mineralization and oil shale respectively), and the amount of fracturing between holes must be maximized for economic reasons. The many problems of mineralization, blast round design, and solution injection and recovery will have to be solved in future studies. The study of blast-produced fracturing provides a logical starting point for analysis of the many faceted in situ mining problem.

This study uses seven laboratory techniques to analyze the fracture state of core removed from the vicinity of several blastholes, relates the results to shot-to-core distances, and compares the techniques.

ACKNOWLEDGMENTS

The authors wish to acknowledge the generous cooperation of the Consolidated Quarries Division of the Georgia Marble Company, Atlanta, Ga. and its Executive Vice President, Nelson Severinghaus, Jr., and its Division Manager, Milton Hamrick. Special thanks are expressed to Bud Pearson for his suggestions and help in solving operational problems at the test site. The authors also wish to thank the Property Determination and Rock Physics research groups of the Twin Cities Mining Research Center and especially Rollie Rosenquist for his technical support and helpful suggestions.

BACKGROUND

Little experimental work has been done on the damage occurring around an explosive detonation in rock; however, the general mechanisms involved are well known. Nearest the explosive charge, there is a shocked and crushed zone (identified in this paper as zone 1) of thickness approximately equal to the blasthole radius and roughly corresponding to the region of shock wave propagation. Beyond the crushed zone is a highly fractured volume (zone 2) containing a network of shear failures probably caused by high level compressional energy from the decayed shock wave. Outside this highly fractured zone the rock contains radial and minor circumferential fracturing and microfracturing produced by the outgoing stress wave (zone 3). Finally, there is a region generally free of blast-produced fractures (zone 4), except where the presence of free faces produce stress wave reflection and tensile slabbing. Atchison (1)[3] describes explosive rock fragmentation process in detail and includes an exhaustive bibliography.

Kutter (13) derived a theoretical model of blast-produced fracturing. He concluded that radial fractures should occur out to six cavity radii from spherical charges and nine radii from cylindrical charges; however, the extension of already existing fractures could occur at far greater distances. His model is based on several assumptions: (1) the fracturing in this region is from a completely confined shot and results from high tangential tensile

[3]Underlined numbers in parentheses refer to items in the list of references preceding the appendix.

stresses; (2) Poisson's ratio is between 0.23 and 0.32; (3) a fixed ratio of 16:1 exists between dynamic compressive and tensile strengths; and (4) the usual simplifications prevail that the rock is isotropic, homogeneous, elastic and stress-free prior to blasting.

Two recent Bureau of Mines studies examined fracturing produced around small diameter blastholes in Bellingham granite and White Pine shale. Olson (18) examined core removed from the vicinity of small explosive charges in granite for evidence of blast-produced damage. Approximately spherical charges of C-4 explosives were used, having a specific gravity of 1.59 and a detonation velocity of 26,400 ft/sec (8.05 km/sec).[4] Using the laboratory techniques of acoustic pulsing and microfracture analysis; evidence of fracturing was found to 1.68 ft (0.51 m) for the 0.25-kg shot and to at least 4.16 ft (1.27 m) for the 2.0-kg blast. These distances are equivalent to 18 and 20 charge radii, respectively. Siskind (22) examined fracture damage in White Pine shale pillars using similar laboratory techniques. Evidence of fracturing was found out to 55 radii from a long cylindrical charge of relatively energetic 60-percent weight-strength extra dynamite and to 15 to 22 radii for AN-FO and the low-density, low-velocity permissible explosives.

Cattermole (6) describes some confined blasting experiments with cylindrical charges and observed a crush zone of 3 blasthole radii, a minutely fractured zone of 10 to 12 radii, and individual radial cracks out to 20 to 30 radii. The rock studied was a tuffaceous pyroclastic rock of the Oak Spring formation; "A rhyolitic to quartz latitic consisting chiefly of altered ash shards and pumice fragments," and the explosive employed was a 60-percent weight-strength dynamite.

---

[4]The prime units in the text, tables, and illustrations of this publication are the U.S. customary units. Where appropriate, the approximate equivalents in the International System of Units (SI) are included in accordance with the rules for introducing modernized metric units established by the National Bureau of Standards ASTM Metric Practice Guide, E380-70. In accordance with the SI convention, a space rather than a comma is used to separate the digits in a metric number such as 15 000. The U.S. customary numbers used throughout the report include commas, where necessary, to separate the digits. The period is used as a decimal point in both SI and U.S. customary unit numbers.

Abbreviations for U.S. customary units and SI units are as follows:

U.S. customary units	SI units
in = inch	kg = kilogram
ft = foot	mm = millimeter
lb = pound	m = meter
	sec = second
	N = newton
	d = darcy
	μ = micro

Published by the Colorado School of Mines in their Underground Explosion Test Program report (7) are some early British formulae:

$$R = 52W^{1/3} \text{ (soft rock)} \quad (1)$$

and

$$R = 40W^{1/3} \text{ (hard rock)}, \quad (2)$$

with R being the radius of rupture (not further defined) in inches and W the charge weight in pounds. The original sources for three relationships are not given. The terms "hard rock" and "soft rock" are also not defined; however, the rock types studied in the Underground Explosion Test Program are sandstone and granite. In International System of Units--(SI) units, the above equations become--

$$R = 1.7W^{1/3} \text{ (soft rock)} \quad (3)$$

and

$$R = 1.3W^{1/3} \text{ (hard rock)}, \quad (4)$$

where R is the radius in meters and W the charge weight in kilograms. By specifying a given explosive, the radius of damage (R) can be computed related only to the original charge radius (r) with the assumption of a spherically shaped charge. For AN-FO with a specific gravity of 0.81, the relationships become--

$$R = 26r \text{ (soft rock)} \quad (5)$$

and

$$R = 20r \text{ (hard rock)}, \quad (6)$$

with the same units of length employed for r and R. For 60 percent weight strength dynamite, equations (3) and (4) become

$$R = 29r \text{ (soft rock)} \quad (7)$$

and

$$R = 23r \text{ (hard rock)}. \quad (8)$$

Derlich (9) studied fracturing and permeability produced by a nuclear shot in granite. He defined the size of crushed and fractured zone using the equation

$$R = 10W^{1/3} \text{ (crushed zone)} \quad (9)$$

and

$$R = 26W^{1/3} \text{ (fractured zone)}, \quad (10)$$

with R being the radii in meters and W the nuclear explosive yield in kilotons (of TNT). Using U.S. customary units, equations (9) and (10) become--

$$R = 3.1W^{1/3} \text{ (crushed zone)} \quad (11)$$

and

$$R = 8.1W^{1/3} \text{ (fractured zone)}, \quad (12)$$

where R are the radii in inches and W the explosive weight in pounds. Employing SI units with R and W being meters and kilograms respectively, Derlich's equations are--

$$R = 0.10W^{1/3} \text{ (crushed zone)} \quad (13)$$

and

$$R = 0.26W^{1/3} \text{ (fractured zone).} \quad (14)$$

Assuming a specific gravity for TNT of 1.56, radii of damage can be computed--

$$R = 1.9r \text{ (crushed zone)} \quad (15)$$

$$R = 4.9r \text{ (fractured zone).} \quad (16)$$

Derlich does not imply that his relationships are valid for small charges; however, it is likely that the difference between equation (16) derived from his work and equation (8) from the Colorado School of Mines study (7) can be attributed to the definition of the "fractured zone." Derlich, defines his crushed zone as having a 14 percent porosity and the fractured zone as being the volume of coarse breakage and intensive fracturing (zone 2), while the School of Mines study refers to the limits of fracturing (zone 3). Analysis of much previous experimental work is complicated by the failure to completely identify what is being considered the "fractured zone."

Atchison (2) investigated damage effects in granite produced by charges of up to 8 lb (3.6 kg). Crushed zone volumes were measured as functions of explosive properties and found to have radii of 3.0 to 4.5 times the blasthole radii. The explosive charges had length to diameter ratios greater than 4:1 and cylindrically shaped crushed zones were assumed.

A similar study was made by Nicholls (16) in volcanic tuff, involving cylindrically shaped charges of up to 29.2 lb (13.2 kg) and having length to diameter ratios of 5:1. Crushed zone volumes were measured and found to be 20 to 35 times the charge volume. If it is assumed that the length of the crushed zone is between one and two charge lengths, the crushed zone radii are in the range of 3 to 6 blasthole radii. A more accurate determination would require measurements of crushed zone shapes or the use of spherically shaped charges. Nicholls also discussed the relationships between the fracture zones and stress conditions produced by blasting, suggesting that the limit of fracturing would be between 2 and 6 times the crushed zone radius. However, no experimental analysis of fracture extent was made.

D'Andrea (8) measured crushed zone volumes produced by small charges of C-4 explosive (S.G. = 1.59) in granite, examining a range of charge sizes from 0.00476 lb (0.00216 kg) to 1.03 lb (0.467 kg). Length to diameter ratios were close to unity, resulting in approximately spherical crush zones. From the data, a radius relationship can be derived--

$$R = 3.6W^{1/3} \text{ (crushed zone),} \quad (17)$$

with R and W being inches and pounds, respectively. This relationship compares quite well with Derlich's equation (11), despite the much different charge sizes involved. Using SI units of meters and kilograms, equation (17) becomes

$$R = 0.12W^{1/3} \tag{18}$$

Several investigators have used geophysical techniques in the field of delineate zones of blast produced-fracturing. Scott (19) examined changes in the physical properties of rock surrounding the Straight Creek tunnel pilot bore. Employing seismic refraction and electrical resistivity, an altered zone extending up to about 15 ft (4.6 m) was found, the first several feet attributed to blasting and deeper occurring changes to stress redistribution. Carroll (5) discusses the Straight Creek work and the role of stress relief in producing the zone of low velocity, additionally describing his own in situ study of downhole seismic sounding in the quartz monzonite and granodiorite of the Climax Stock at the U.S. Atomic Energy Commission Test Site near Mercury, Nevada. He found an altered zone ranging from zero to approximately 8 feet in thickness with much of the data suggesting that blast produced damage existed to a depth of 2 to 4 feet. Carroll (5) does not specify the proximity of the analysis holes and the tunnel perimeter blastholes or the blasthole sizes. Miller (14) applied seven field techniques to determine the extent of fragmentation produced by blasting in an oil shale deposit. He found that the seismic data analysis, which consisted of evaluation of arrival times, amplitudes, and record quality provided the best indication of fracturing of the techniques employed. The blast consisted primarily of five 6-1/2-inch-diameter vertical shotholes, arranged in a square array with a single center hole. The fragmented zone was found to be approximately 95 ft (29 m) in diameter; however, the degree of fracturing within the fragmented zone could not be determined by the seismic analysis techniques. Recovery cores were drilled at distances from the closet blasthole of 26, 13, and 8 ft. Some information about the fracture state of the core can be inferred by the fines that were lost in the drilling fluid, with core losses of 2, 7, and 30 percent, respectively.

Two other areas of blast-produced damage to rocks have been extensively studied. These are the analysis of shock effects (producing zone 1 damage) and air and ground vibrations (zone 4). Because the present study is concerned with the other two damage zones, no description of these blast effects will be discussed except to refer to an excellent summary article by Short (20) describing shock processes in geology and the final of a series of Bureau of Mines Reports of Investigations on vibrations produced by underground blasting (21).

Knowledge of the extent and degree of fracturing produced by blasting is of primary importance in the evaluation of rock competency both for the control of damage effects in mining and excavation and for the use of explosives for fragmentation for situ mining.

EXPERIMENTAL PROCEDURE

Test site

The Lithonia granite quarry located at Rock Chapel Mountain has been the site of several previous studies including blast effects (2), measurement of ground stresses (11-12, 17), and presplitting experiments in the presence of a static stress field (15). The rock is most accurately called a "granite-gneiss" but in previous work has been labeled Lithonia granite, Lithonia gneiss, and Lithonia granite-gneiss. Throughout this report, the foliated granite will simply be referred to as Lithonia granite. Figures 1, 2, and 3 show the site location, quarry geometry, and view of the test site area. The three shotholes and the control hole (H-100) locations are indicated in figure 2.

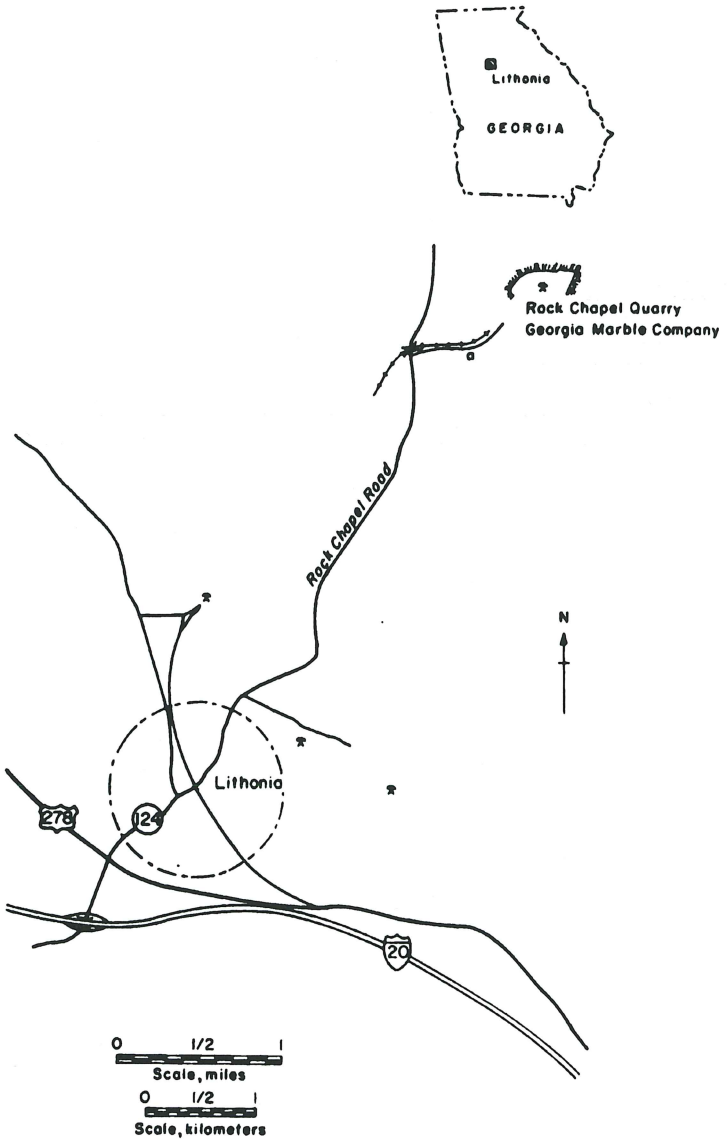

FIGURE 1. - Quarry location map.

Rock Description

The rock is a fine to medium grained biotite granite, highly folded and sheared, and containing garnet and magnetite crystals (10). Aplite and quartz veins commonly cut across the foliation. Thin section model analysis gave an average composition of 35 percent microcline, 30 percent oligoclase, 25 percent quartz, 5 percent biotite, and traces of muscovite, apatite, and epidote (17). Shown in figure 4 is a piece of recovered core, showing a fracture, foliation, and microstructure.

Two major shear zones strike N 10° - 70° W with the axes of flow folds ranging from N to N 20° E and plunging 10° to 25° N (10). A detailed analysis of the genesis of the granite-gneiss is given by Blair (3),

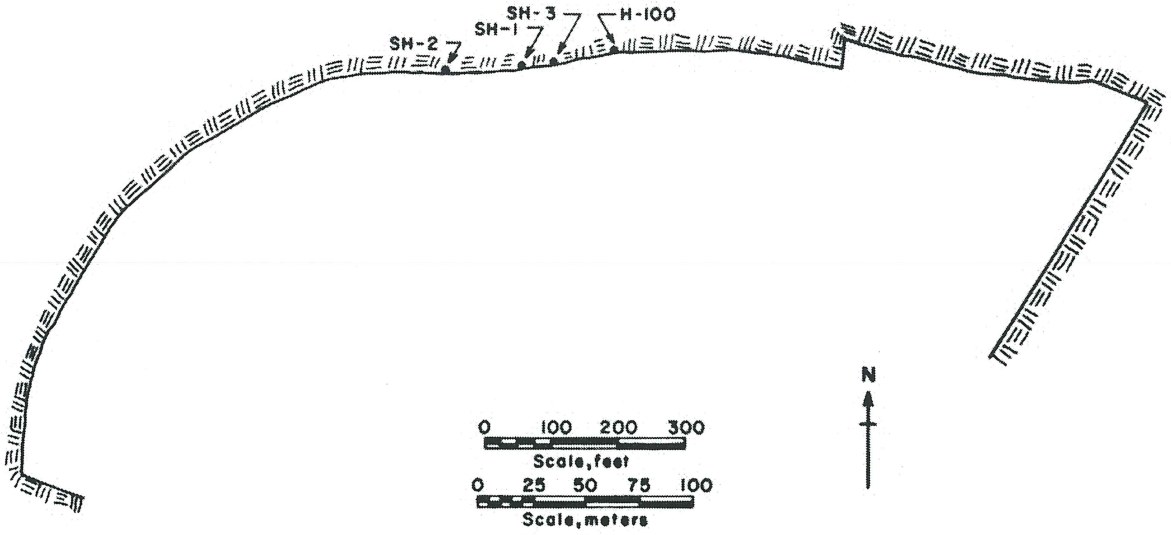

FIGURE 2. - Plan view of quarry at time of study (January 1972).

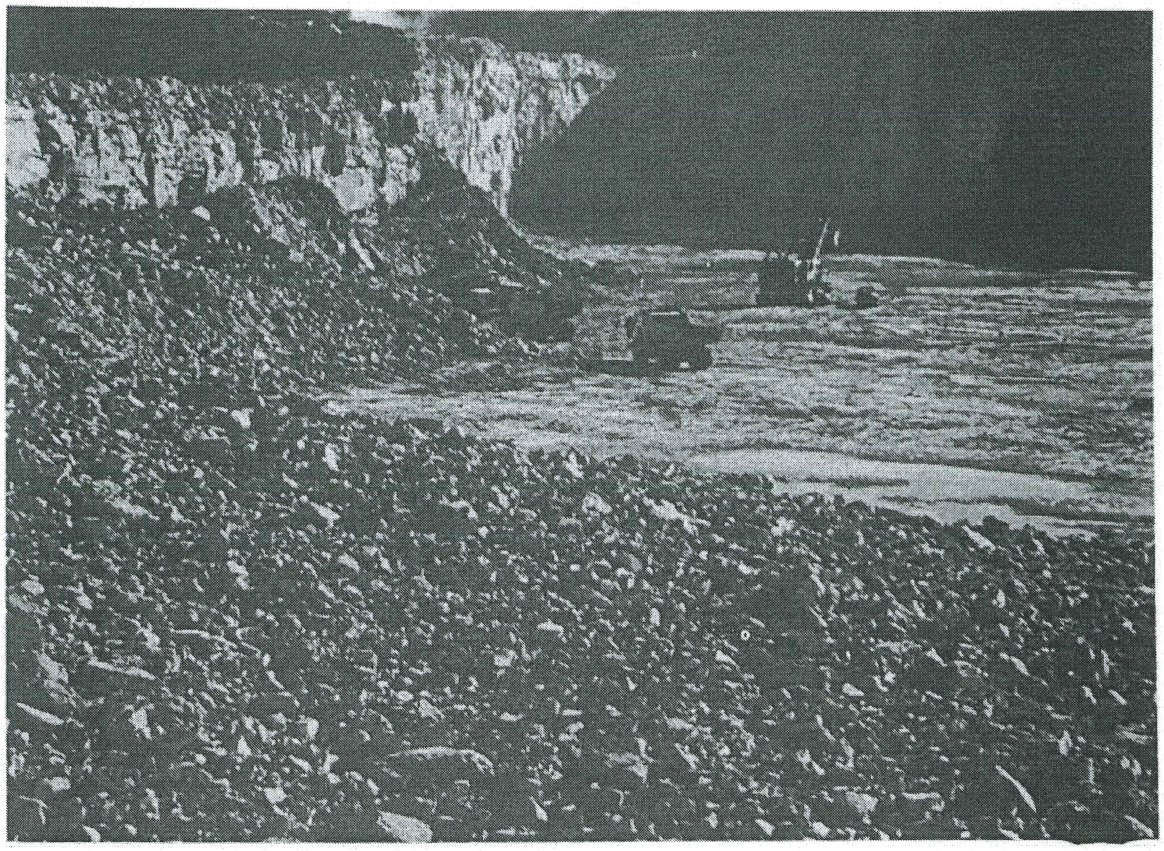

FIGURE 3. - Overall view of quarry and test site.

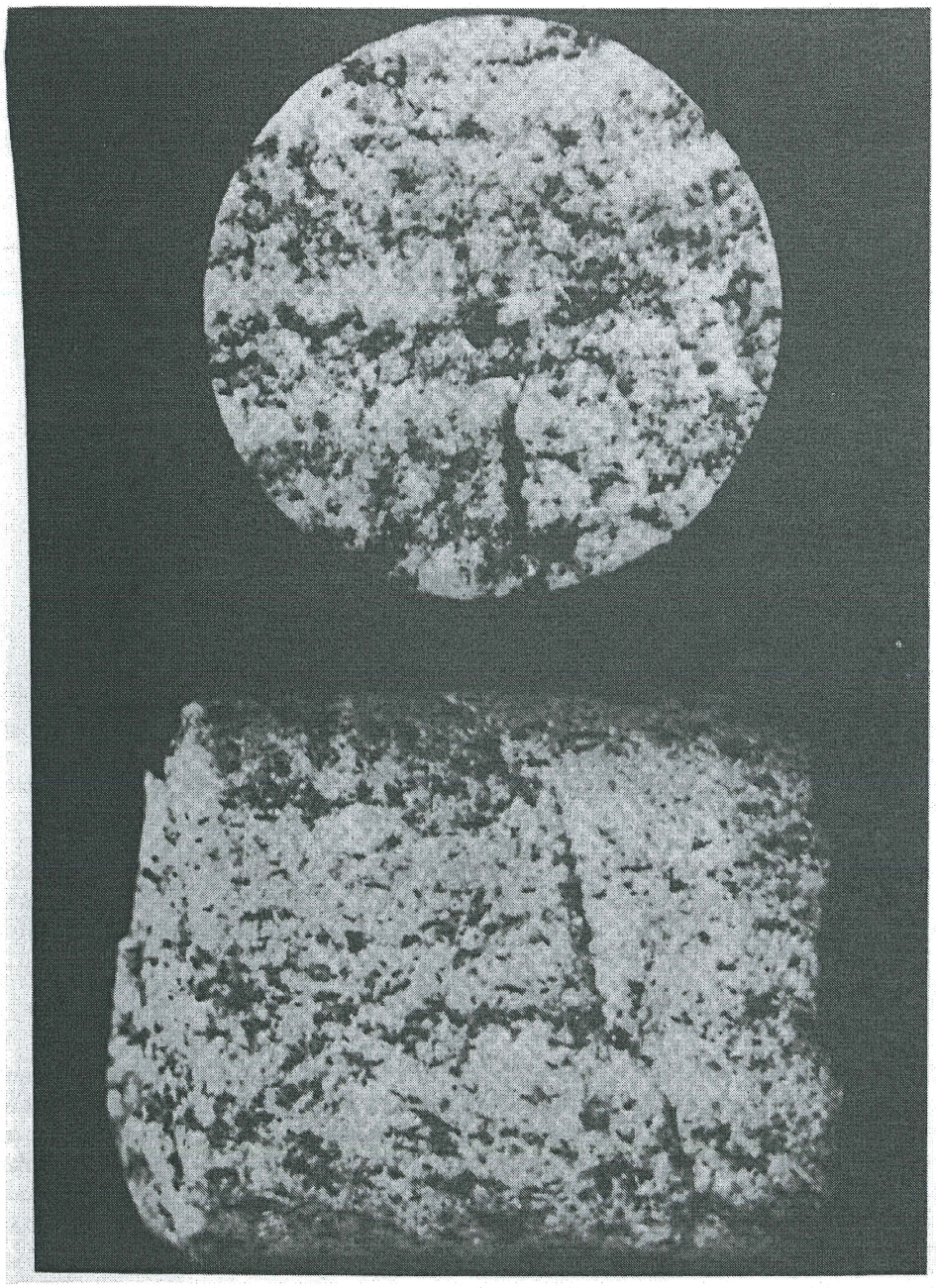

FIGURE 4. - Section of core, Lithonia granite.

and physical properties of the rock were measured by previous investigators from core samples (unless specified otherwise) and are given in table 1 (2-3). Young's modulus and modulus of rigidity were determined using sonic techniques.

TABLE 1. - Physical properties of Lithonia granite

	U.S. customary	SI units
Specific gravity.....	2.63	2.63
Weight density.....	164 lb/ft^3	2 630 kg/m^3
Longitudinal propagation velocity, in situ.....	18,200 ft/sec	5 550 m/sec
Longitudinal bar velocity....	9,000 ft/sec	2 740 m/sec
Tensile strength.....	450 lb/in^2	3.10 x 10^6 N/m^2
Compressive strength.....	30,000 lb/in^2	207 x 10^6 N/m^2
Modulus of rigidity.....	1.5 x 10^6 lb/in^2	10.3 x 10^9 N/m^2
Young's modulus.....	3.0 x 10^6 lb/in^2	20.7 x 10^9 N/m^2
Poisson's ratio in situ.....	.26	.26

Several studies have been made of the stress conditions and anisotropy of the Lithonia granite. Hooker (11) used borehole deformation gages to measure stress conditions in a near-surface horizontal plane and found maximum secondary compressive stresses (P) of 965 to 3,023 lb/in^2, with a mean of 1699 lb/in^2 (6.66 x 10^6 to 20.8 x 10^6 N/m^2, mean of 11.7 x 10^6 N/m^2) at directions ranging from N 40° E to N 70° E, mean of N 56° E. Minimum secondary compressive stresses (Q) ranged from 503 to 1,390 lb/in^2, with a mean of 978 lb/in^2 (3.47 x 10^6 to 9.58 x 10^6 N/m^2, mean of 6.76 x 10^6 N/m^2).

Presplitting experiments were made in the Lithonia granite by Nicholls (15). Fracturing was attempted along a line at a strike of N 56° E, selected to coincide with the average direction of the maximum stresses (P) measured in the local vicinity. A series of parallel fractures resulted, trending N 48° E. An identical line of charges was placed to intersect the first array at 90° and failed to produce visible damage to the rock.

Norman (17) discusses relationships between the ground stresses and geologic structure at the Rock Chapel Mountain site. In addition to summarizing previous work at the quarry, he examined microstructure and found a preferred direction of microfractures of N 30° W to N 45° W. These fractures were aligned approximately normal to P and attributed not to blast produced damage but to tensile stressed produced by release of the rock from high compressive loading.

As part of the present study, an oriented specimen was recovered for measurement of anisotropy. Using the method developed by Bur (4), the rock was found to be orthotropic with an anisotropy (A) of 27.2 percent, computed from the relationship--

$$A = \frac{Vmax - Vmin}{(Vmax/2)+(Vmin/2)}. \qquad (18)$$

The direction of Vmax is N 40° E.

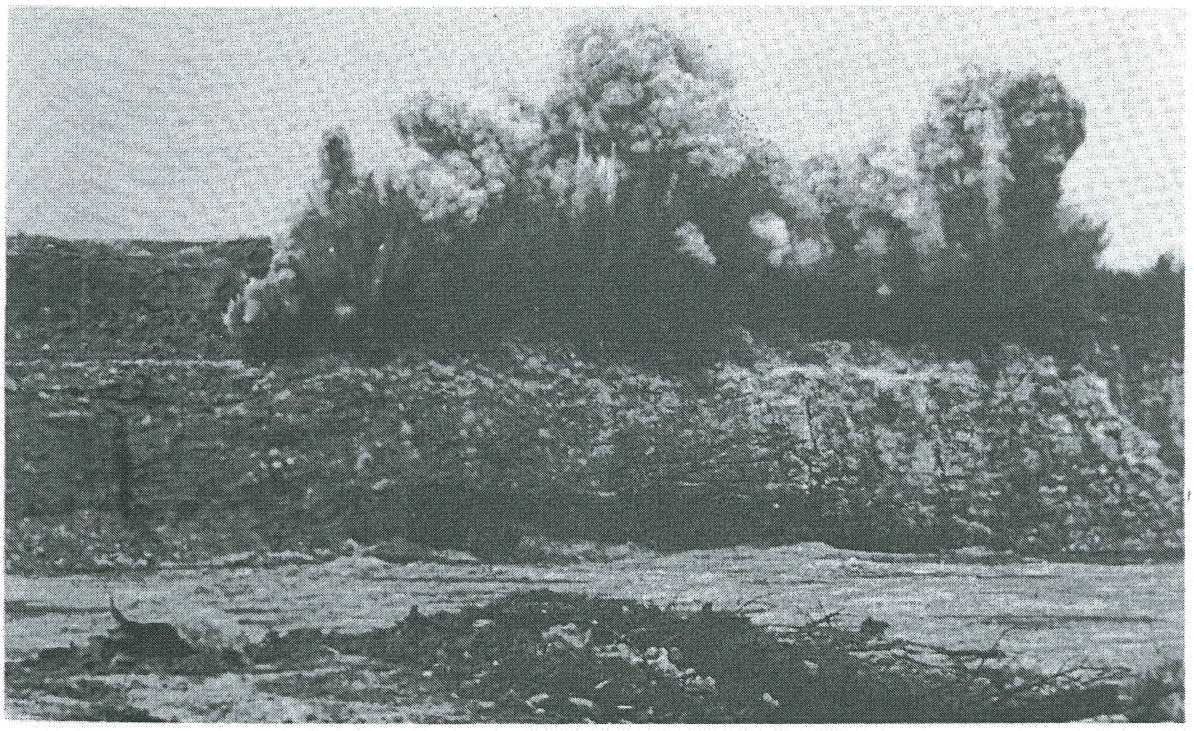

FIGURE 5. - Quarry production blast.

Blasting

Production blasting at the Rock Chapel Mountain quarry is done with 6-1/2-inch-diameter vertical holes of AN-FO in the 60- to 80-ft (18 to 24 m) bench at a spacing of approximately 16-ft (4.9 m). Five feet of subdrilling is used and the holes are bottom initiated with a primer of TOVAL[5] dynamite. Figure 5 shows a quarry production blast fired at the time of the study. The area from where the blast-damaged core was recovered had been shot the previous spring; however, the face appeared fresh and unweathered as contrasted with a much older upperlevel bench.

Figure 6 shows an overall view of the truck in place for drilling at the rock bench.

Recovery Core Drilling

Explosively damaged core was recovered by diamond drilling into the bench face starting in the blasthole cast, or trace of the blast-crush zone. A total of 91.2 ft (27.8 m) of AX size core (1-3/16-inch-diameter) was recovered including a single control hole (H-100) drilled from rock between two blastholes. All the blastholes were vertical and the core drilling was done horizontally (or perpendicular to the blastholes) at various azimuths and heights above the quarry floor. Table 2 summarizes the recovery core drilling.

[5]Reference to specific brands or trade names is made for identification only and does not imply endorsement by the Bureau of Mines.

TABLE 2. - Recovery core drilling data

Blasthole	Recovery hole	Height above quarry floor		Azimuth	Distance from bench face or blasthole (depth)			
					Beginning of recovered core		End of recovered core	
		Inches	m		Inches	m	Inches	m
SH-1	H-1	74	1.88	N 39° W	6.5±1.5	0.17±.04	104.5	2.65
	H-2	63.5	1.61	N 37° W	10.5±1.5	.27±.04	60	1.52
	H-3	53.5	1.36	N 37° W	12.5±1.5	.32±.04	81	2.06
SH-2	H-1	78	1.98	N 41° W	11±2	.28±.05	76.5	1.94
	H-2	73	1.85	N 41° W	11±2	.28±.05	60	1.52
	H-3	68	1.73	N 41° W	9.5±2	.24±.05	64.5	1.64
	H-4	63	1.60	N 41° W	9.5±2	.24±.05	65	1.65
SH-3	H-1	84	2.13	N 64° W	14±2	.36±.05	100.8	2.56
	H-2	79	2.01	N 64° W	12±2	.31±.05	96	2.44
	H-3	84	2.13	N 43° W	16±2	.41±.05	66	1.68
	H-4	79	2.01	N 43° W	13±2	.33±.05	86.5	2.20
	H-5	79	2.01	N 23° W	13±2	.33±.05	56	1.42
	H-6	70	1.78	N 23° W	15±2	.38±.05	80	2.03
	H-100	80	2.03	N 40° W	0	0	117	2.97

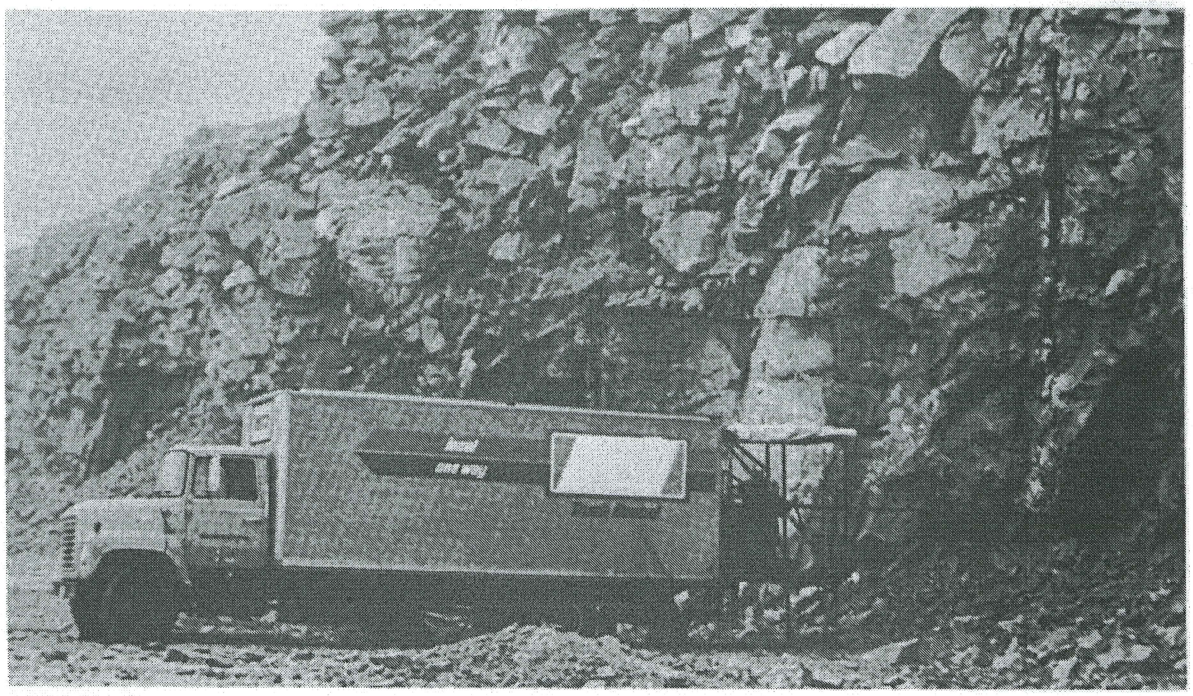

FIGURE 6. - Drilling truck and quarry bench.

A Sprague and Henwood model 35H drill with a 15.5 HP air-cooled diesel was used for coring. Since the drill has no elevation adjustments it was mounted on the modified power lift tailgate of the truck. The hydraulic system of the truck was not capable of lifting the tailgate drill, drill steel, and operators, and maintaining a precise horizontal attitude. Therefore, a 3-1/4- by 48-inch air cylinder was mounted on the back of the tailgate drilling platform to assist the trucks hydraulic cylinder, and controls for both devices were operated simultaneously by a single person. The vertical movement of the drilling platform included a 5-inch arc course, compensated for by the use of a steel wheel mounted on the bottom of the air cylinder and rolling on a steel plate. In addition, safety legs and chains were used during drilling. Figure 7 shows the drilling platform, air cylinder, N gas tank and overhead safety shield. Shown in figure 8 is the drilling of recovery hole SH-1, H-3. A template had been used to collar and space the recovery hole from previous ones drilled higher up and into the same blast hole. Figure 9 shows a close-up of the recovery drilling into SH-3, where a total of six cores were recovered at three different azimuths.

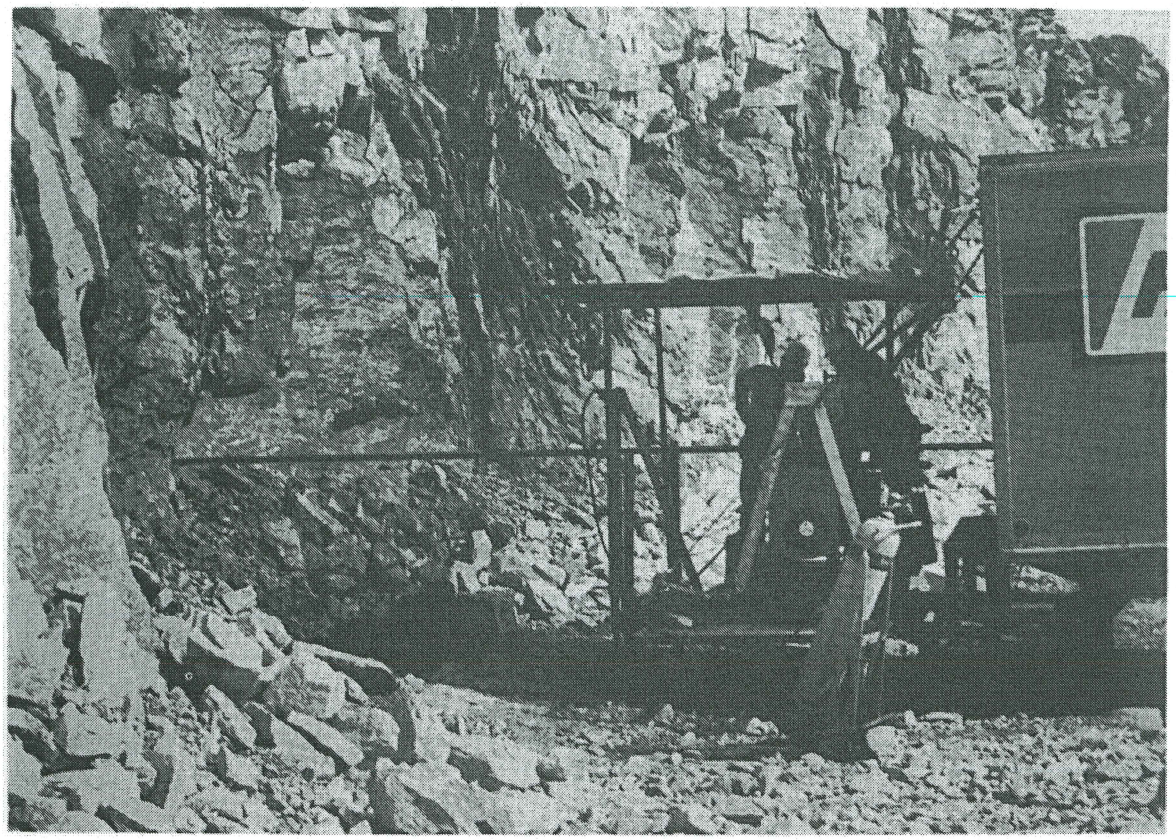

FIGURE 7. - Drilling rig.

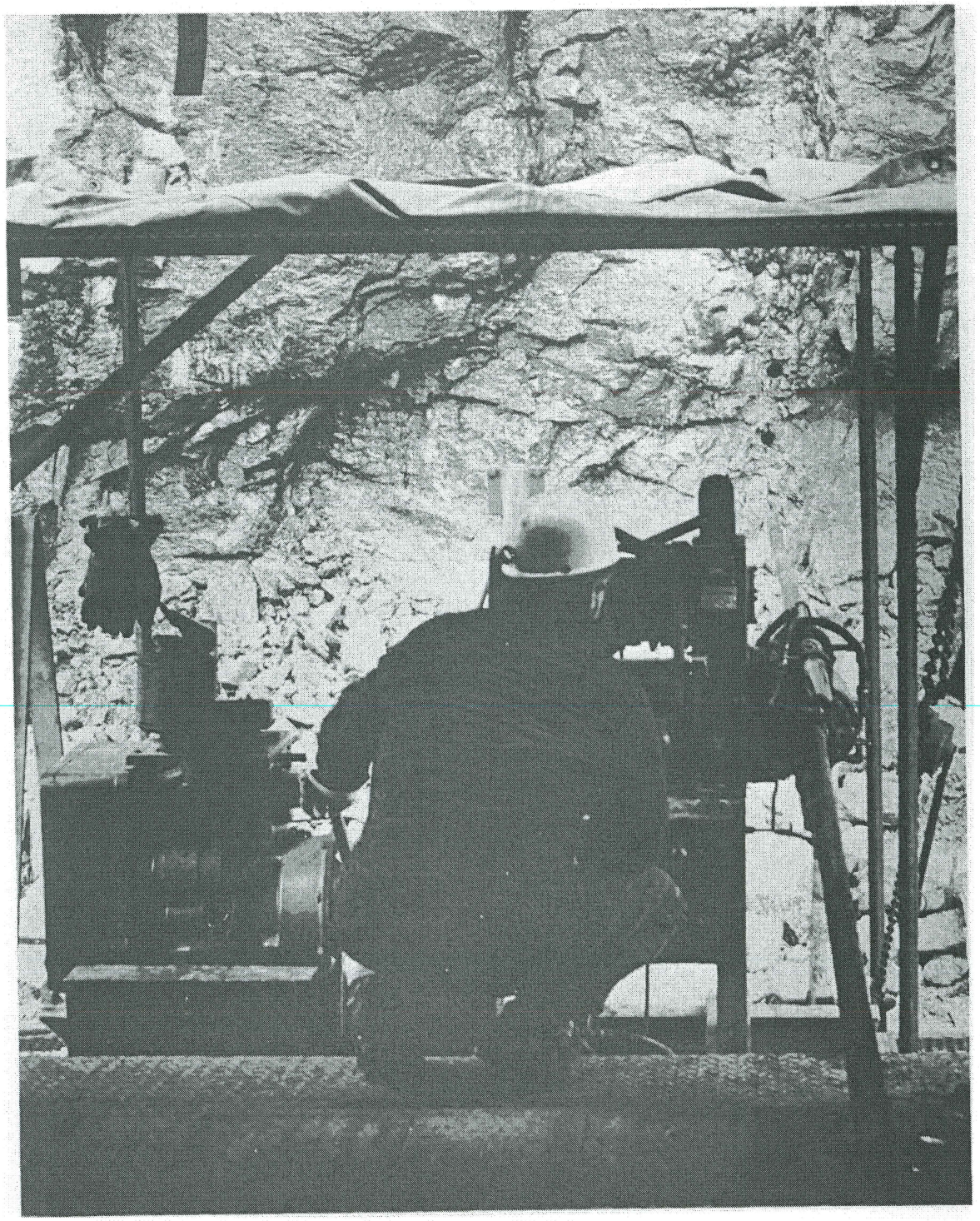

FIGURE 8. - Drilling shothole No. 1.

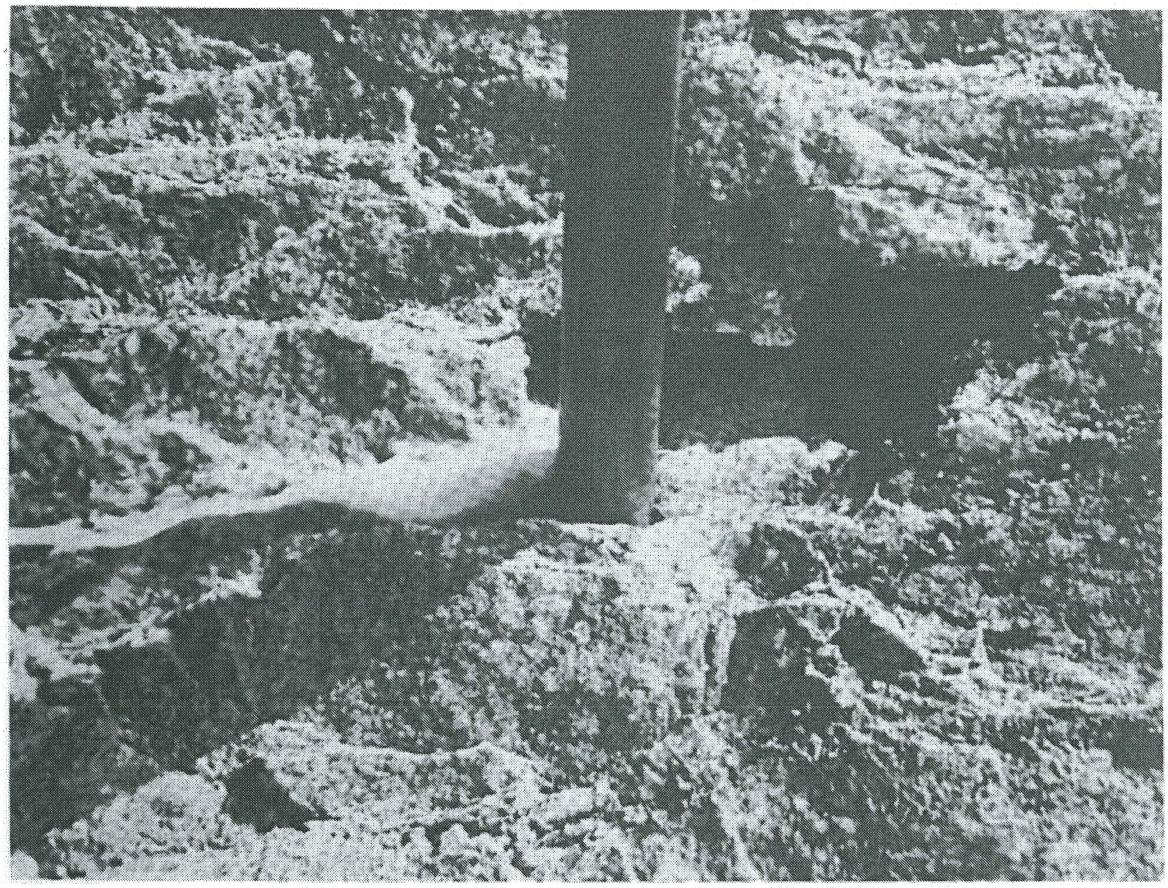

FIGURE 9. - Closeup of shothole No. 3.

The close-spaced fractures in this crushed zone boundry region are visible. A plan view of the 13 recovery holes showing depths and azimuths is shown in figure 10. Ten carat diamond weight AX bits were used, giving an initial advance rate of 2 in/min (51mm/min) and a steady rate of approximately 1 in/min (25mm/min) in the hard crystalline rock.

Damage Analysis Techniques

A total of six laboratory analysis techniques were used to evaluate the fracture state of the 167 specimens of recovered core. The first selection consisted of 38 small and fractional core sections, analyzed for porosity using helium gas porosimetry techniques. These pieces were too small for additional study. Fifty 2-3/8-in long pieces were then prepared for axial compressive strength testing, with the simultaneous measurement of Young's molulus. The large sampling of 80 pieces was then made and permeabilities measured. The method used involved the percolation of fluid (in this study water) axially through the specimen, under pressure. Permeabilities were calculated from pressure, specimen dimensions, and time required for passage

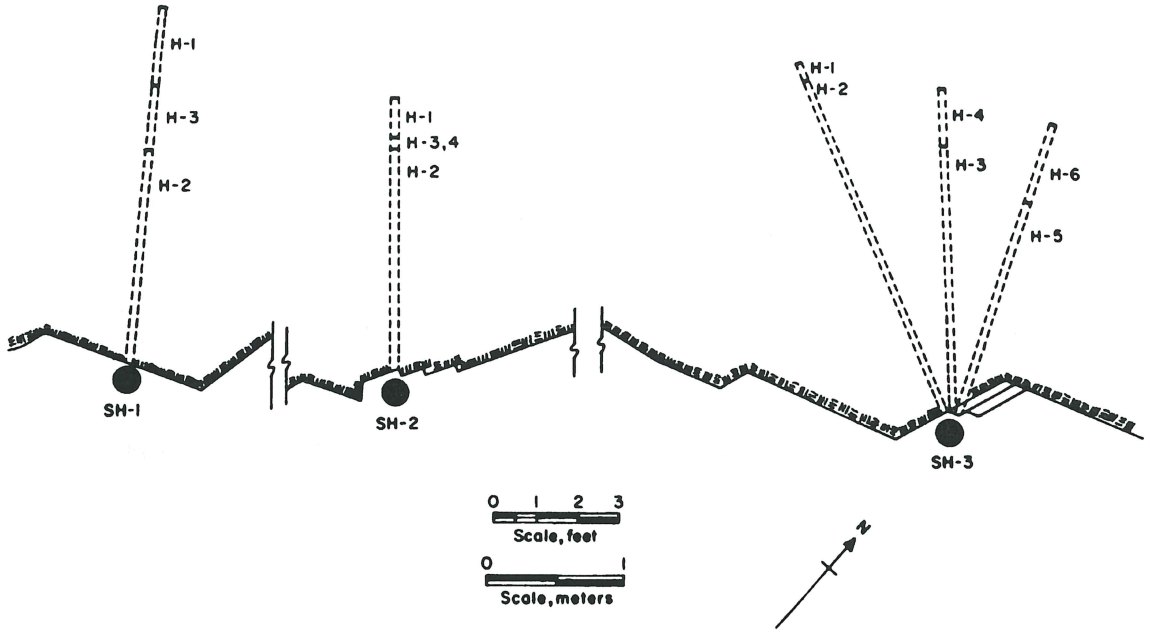

FIGURE 10. - Plan view of shothole recovery drilling.

of the water. Excluding one specimen which broke, the large set of core pieces was then examined in an acoustic bench for anomalous diametrical travel times as in the two previous studies (18, 22). Each one-inch core piece was pulsed four times across the diameter at 45° intervals and the mean, minimum, maximum and range of acoustic velocities were computed. A selection of 45 of the 79 test pieces was made for additional porosity measurements, and then all 79 specimens were destructively tested by loading across the diameter between flat platens as in Brazilian strength testing. It was felt that this technique would be sensitive to axially running fractures, and to insure no bias due to alignment with foliation banding, specimens were oriented in the testing machine at random. The rock was expected to have strength-anisotropy, and that the effect of blast-produced fracturing would be evident as a strong overall reduction in Brazilian strength. Failure was defined in units of load per unit length, and no attempt was made to relate the measurements to tensile strength.

All of the data from the laboratory tests were plotted against core depth to produce property logs. As in a previous study (22), core length histograms were also made, giving a "rock quality designation" (RQD) of the number of fractures (pieces) per unit length. As in the previous study, 1-foot unit lengths were used.

EXPERIMENTAL RESULTS

Analysis of Damage

The analyses of the blast-produced damage in the 13 recovery cores are shown in figures 11 through 23. Each figure contains some measured physical property versus distance from a blasthole center, defined as "depth." In all cases, some crushed zone rock was missing and estimates of the depths of the first pieces of recovery core had to be made. A Brunton compass was used to sight along the blasthole cast and the uncertainty of the exact depth of the beginning of the recovered core is shown in table 2, being ± 2.0 inches for most of the holes.

The blast-damaged core was assumed to be in one of three states; multiply-fractured with cracks running several directions, multiply- or singly-fractured with cracks in only one direction, and totally unfractured. These states roughly correspond to zones 2, 3, and 4, respectively, discussed previously. The existance of veins, inclusions, and voids constitutes a fourth state of competency. All individual laboratory measurements are listed in the appendix.

Porosity Measurements

Porosity measurements are given in figure 11. The summary graph shows measurements from all the blast-damage core with data from the undamaged control core shown for comparison. Most notable are both high and low anomalous values close to the blast, with high porosities expected to result from blasting and also from any conditions such as any pre-existing voids fractures, and veins. The absence of high values beyond about 24 inches (0.61 m), or 7.4 blasthole radii, and the agreement between these values and the control hole porosities, suggest that this is competent and undamaged rock. The additional problem of the low values at shallow depths probably results from pores being closed by blast-produced dust or partial crushing.

Permeability Measurements

The permeability measurements are shown in figure 12 and contain a great amount of scattered high values, contrasting sharply with the uniform values (ranging between 5 and 10 μd) for the control hole. These high permeabilities at great depths are most likely unrelated to the blasting; however, the absence of low values closer than about 23 inches and the preponderance of high values of permeability suggest the existance of many open fractures.

Closer than 20 inches (0.51 m) or 6.2 blasthole radii, the permeabilities of the core specimens range from 30 to about 1000 μd with a median value of approximately 150 μd. For oil and gas well reservoirs, permeabilities below 5000 μd are considered "tight or dense."

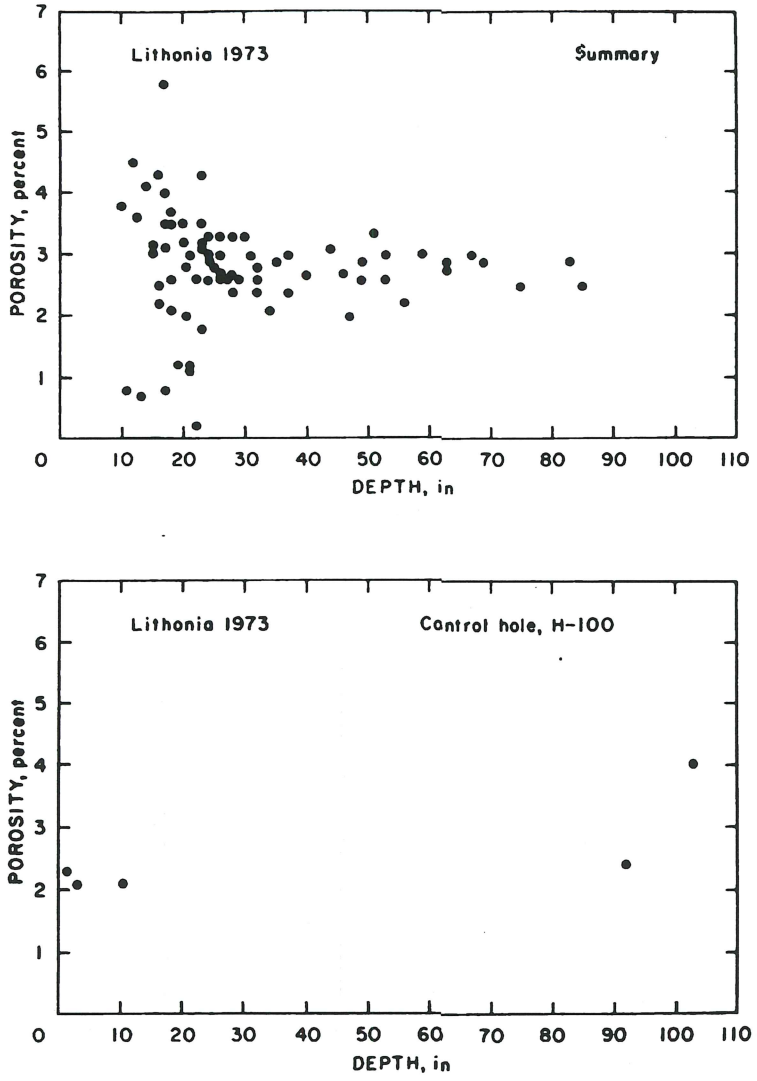

FIGURE 11. - Recovery core analysis, porosity.

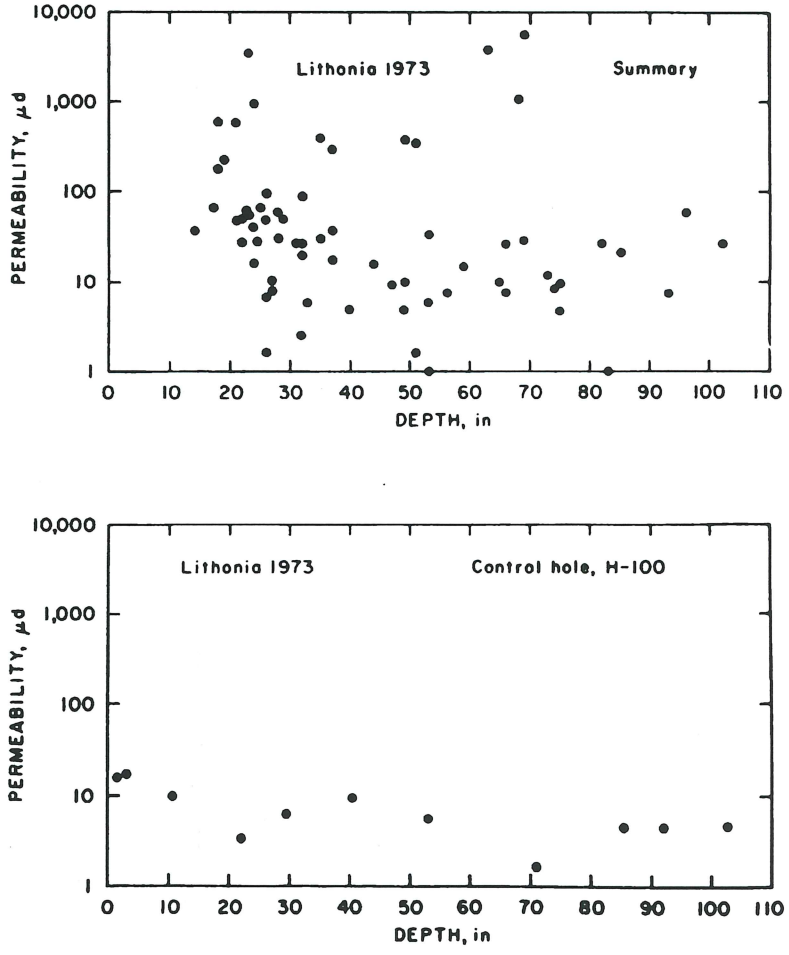

FIGURE 12. - Recovery core analysis, permeability.

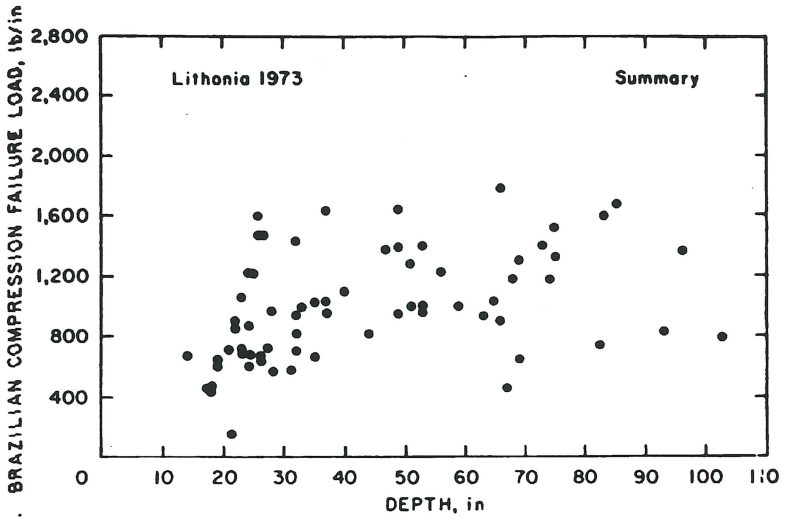

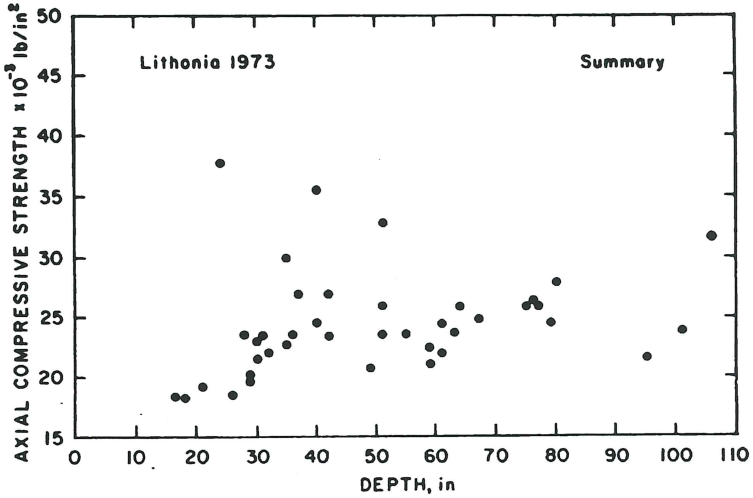

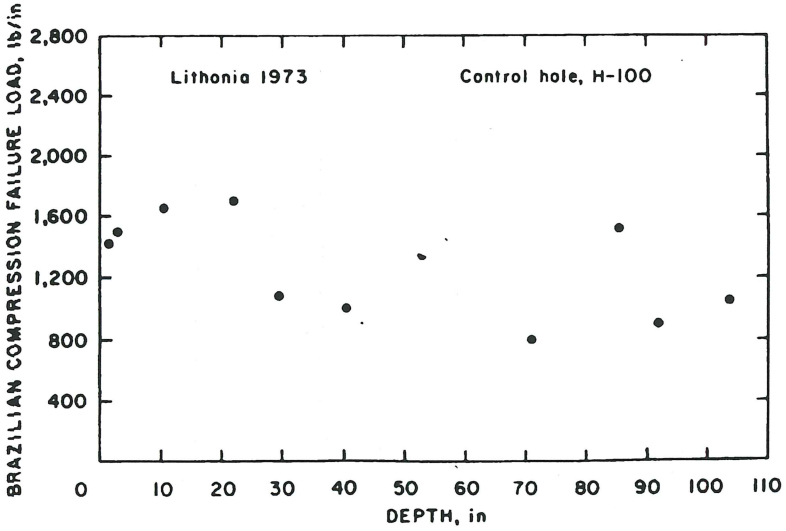

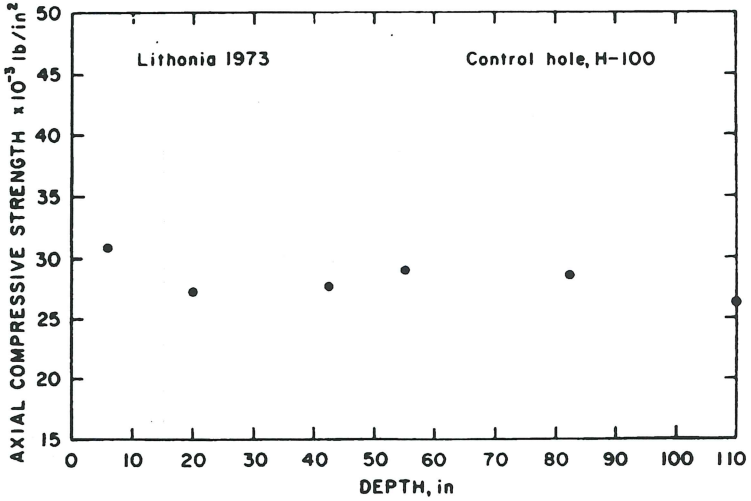

FIGURE 13. - Recovery core analysis, Brazilian strength.

FIGURE 14. - Recovery core analysis, axial compressive strength.

Brazilian Strength Measurements

The strength of the core in diametrical compression loading was expected to be a sensitive indicator of the existance of longitudinally oriented fractures. Unfortunately the results as shown in figure 13 contain a great amount of scatter complicating the interpretation. Much of the scatter is probably due to the random orientation of the specimens between the platens. A larger sampling, particularly of control hole core, would have allowed the determination of the strength-orientation relationships and property measurements in specific directions; however, useful interpretation would have required that absolute orientation of the recovery core would be maintained. Examining maximum values measured, it appears that standard values[6] of strength are reached at a depth of 25 inches (0.64 m; 7.7 blasthole radii). The many low-strength values below about 35 inches (0.89 m; 10.8 blasthole radii) suggests the existence of scattered fractures.

Axial Compressive Strength Measurements

Unlike the Brazilian strength tests, the uniaxial or conventional compressive strength measurements for the control hole core are very uniform, approximating 28,000 lb/in^2 (193×10^6 N/m^2). However, except for a few scattered measurements, the compressive strengths of the blast-damage core as shown in figure 14 do not attain this standard value. Other than one very high strength value at a depth of 24 inches (0.61 m), there are three ranges of values: (1) Low strength out to 28 inches (0.71 m; 8.6 blasthole radii); (2) intermediate strengths from about 28 to 37 inches; and (3) scattered high and medium compressive strength values at depths greater than 37 inches (0.94 m; 11.4 blasthole radii).

Young's Modulus Measurements

Shown in figure 15 are the Young's modulus measurements made simultaneously with the axial compressive strengths. The standard values attained from the control hole core are highly uniform, but unlike the compressive strength values their average of 6.4×10^6 lb/in^2 is not in agreement with the reported value in table 1 from previous investigators. Standard values of Young's modulus for the blast-damage core are attained at approximately 28 inches (0.71 m; 8.6 blasthole radii) and at depths greater than 32 inches there is a total absence of low values.

---

[6]Standard value is the normal value of each measured property with no blast damage, as measured from the control hole core or from other measurements. Deviation from the standard value is an indication of blast damage

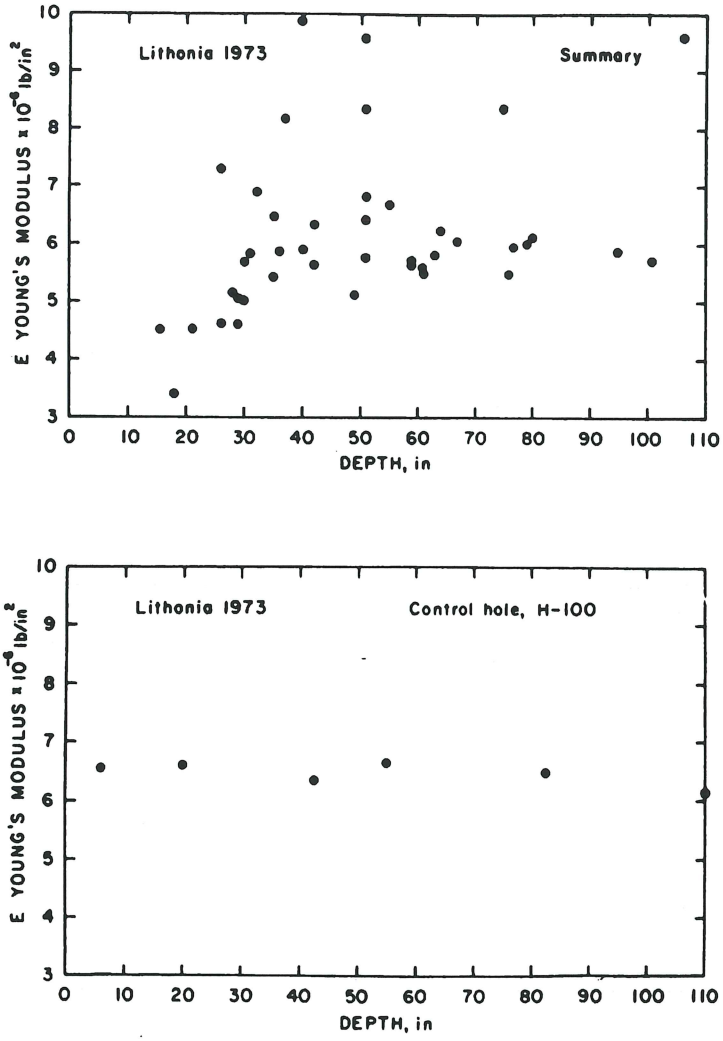

FIGURE 15. - Recovery core analysis, Young's modulus.

Acoustic Pulse Velocity Measurements

Figures 16 through 20 show the results attained from measuring the acoustic pulse diametrical travel-times of the samples of recovered core. Shown in figure 16 are the idealized results that should be found in a uniform isotropic blast-fractured rock, using the current techniques. Each sample is pulsed in four directions giving four values for pulse velocity (computed from diametrical travel-times), and figure 16 shows four methods for analyzing the measurements. The "mean" is attained by averaging the four values, with multiply-oriented fractures lowering several or all of the travel times and having the strongest influence on the mean velocity. Maximum velocity is simply the highest of the four values measured, and low values of the maximum are an indication of multiple-directional fracturing. By contrast, "minimum velocity" can indicate single-direction fracturing with the direction of minimum velocity being normal to the fracture plane. These idealizations result from the expectation that a single fracture will lower pulse velocities the most in the direction normal to the fracture and can be detected by seeking the minimum value (of the four measurements). However, all four pulse velocities from a single core piece will be low only if the core is fractured in several directions. The "range" is simply the maximum of the four measurements minus the minimum for each sample and should be highest with extensive single-direction fracturing. A finite value of the range at great depths is indicated and is a result of anisotropy and experimental scatter. Ideally, the range at large distances from disturbing influences should be zero.

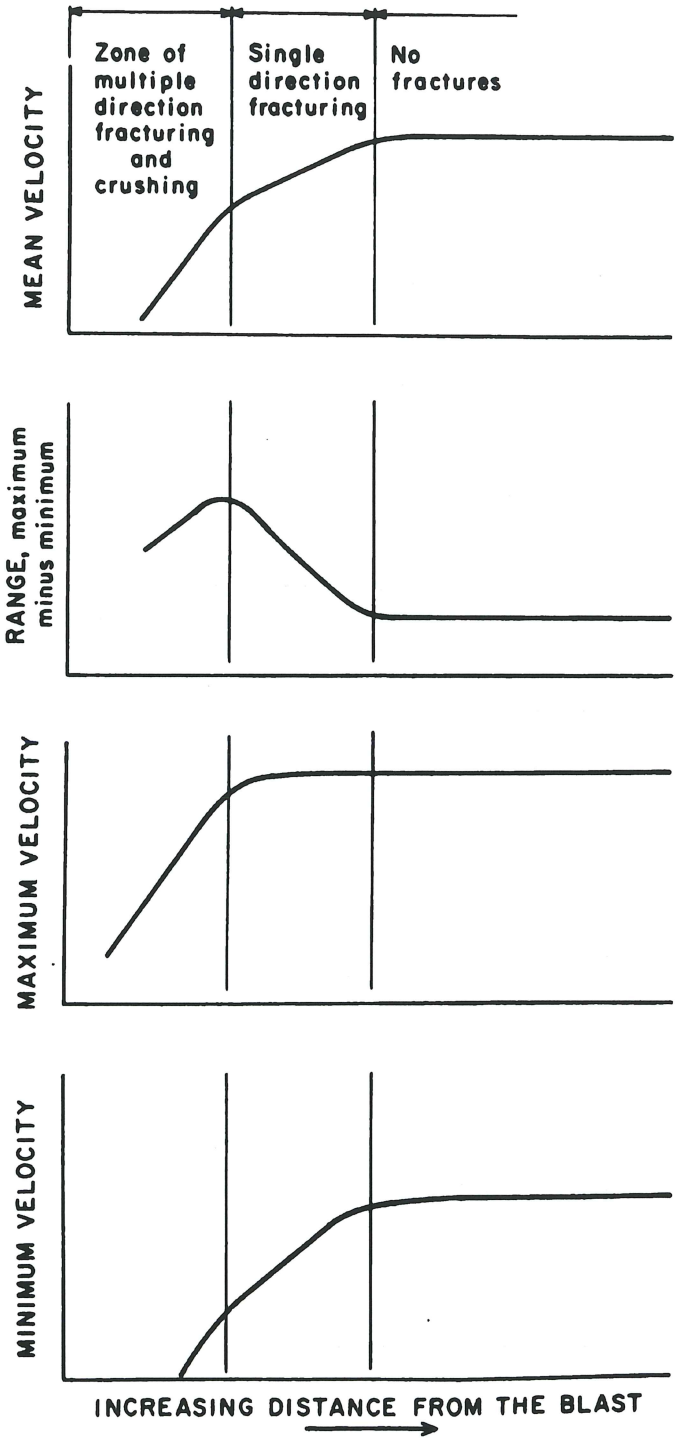

FIGURE 16. - Recovery core analysis, idealized acoustic-pulse velocity measurements.

Shown in figure 17 is the mean acoustic velocity data as measured from the blast-damaged core and the undamaged control core. Two effects are noticeable: standard values are reached at a depth of 27 inches (0.69 m; 8.3 blasthole radii) and there are many low values occurring below about 47 inches (12.0 m; 14.5 blasthole radii). There is little scatter in the control hole data. The blast-damaged core velocities are very sensitive to depth and approach the standard value as expected. The range of acoustic velocity data as shown in figure 18 fails to give any strong indication of fracturing or to agree with the expected ideal behavior. There is a great amount of scatter in both the summary graph and control hole data, from the existence of some kind of combination of fractures, voids, inclusions, inhomogeneities, stresses, anisotropy, and so forth. Notable are both the high and very low values of the range below about 40 inches suggesting that the single-directional-fracturing indicated by the other analyses techniques may be partially masked by the anisotropy. Recall that the recovery holes were drilled approximately N 40° W, approximately normal to the direction of Vmax (N 40° E). Consequently, the lowering of the pulse velocity across the radial fractures (fractures running longitudinally down the core) will either add or partially cancel out the essentially horizontal Vmax, depending on the fracture orientation.

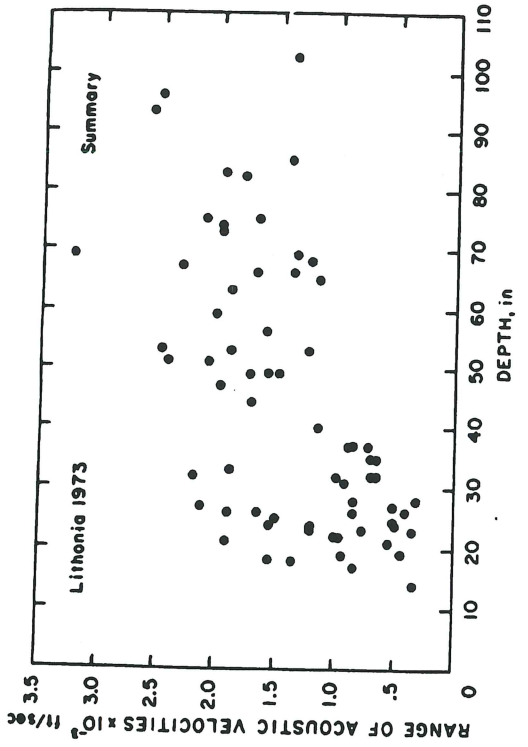

FIGURE 18. - Recovery core analysis, range of acoustic velocities.

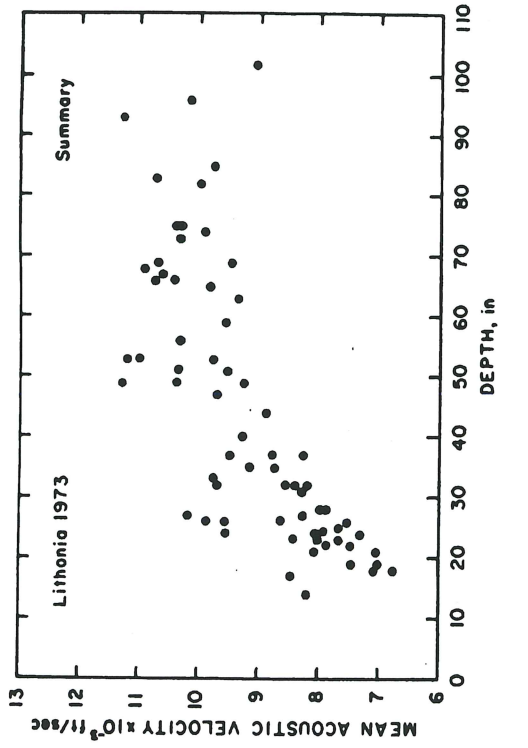

FIGURE 17. - Recovery core analysis, mean acoustic velocities.

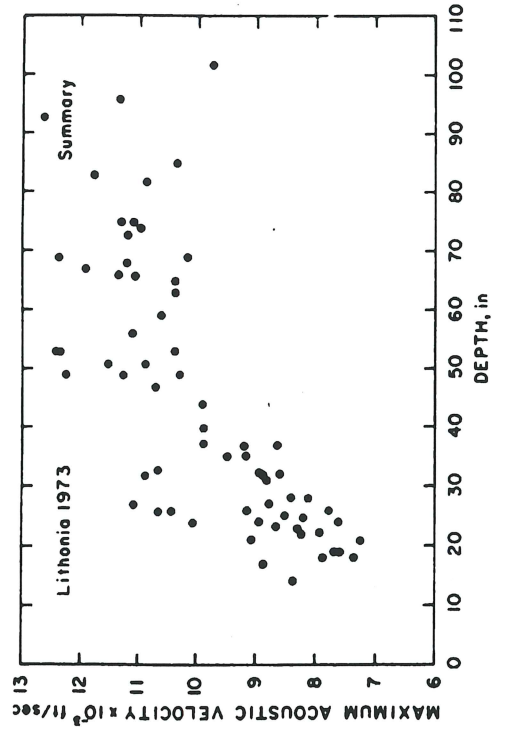

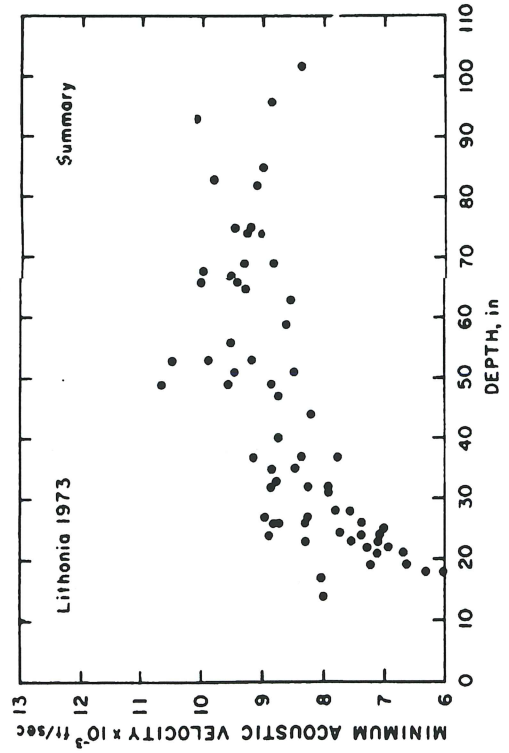

FIGURE 19. - Recovery core analysis, minimum acoustic velocities.

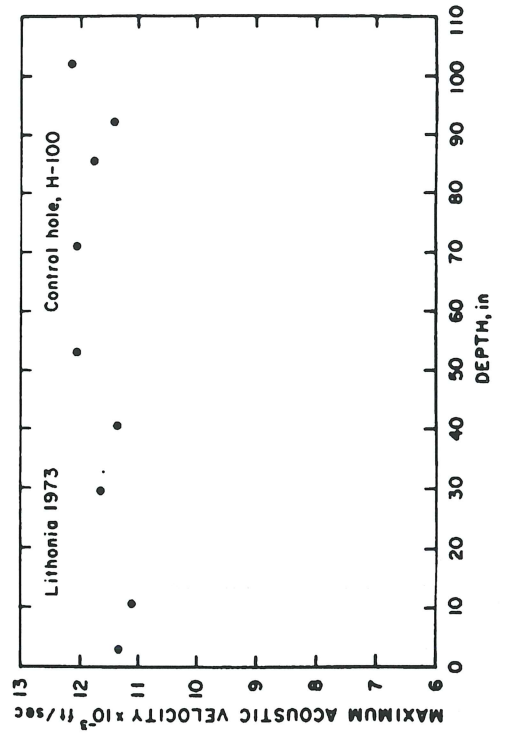

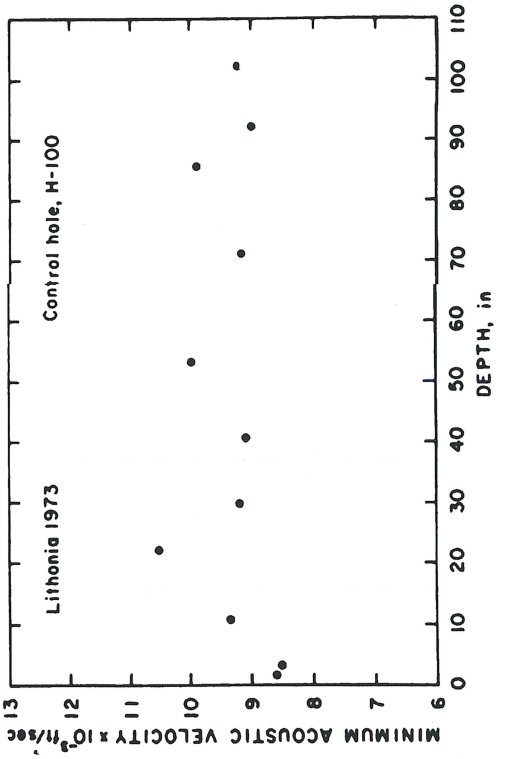

FIGURE 20. - Recovery core analysis, maximum acoustic velocities.

The minimum and maximum values as shown in figures 19 and 20 do not show the predicted idealized contrast. They are surprisingly similar in both having an absence of low values at depths greater than 45 inches (1.4 m; 13.8 blasthole radii), and both having some cores with measured values corresponding to normal, or unfractured rock, occurring at about 25 inches (0.64 m; 6.7 blasthole radii). From these results, it is likely that the core from depths greater than 20 inches is not multiple-directionally fractured. However, out to about 25 inches essentially all the core is fractured, between 25 and 45 inches there is scattered fracturing, and beyond 45 inches there is little or no fracturing.

Core Logs

The core recovery data of figure 21 is obtained at the time of drilling and substantiates the laboratory damage analyses. The control hole indicates that weathering and near-surface effects produce small pieces within the first foot of recovered core. The summary core fracture log is an average of all the blast-region core and contains many small pieces within the first 2 feet and a smaller amount of fracturing in the 3d foot. Above 36 inches (the third foot), the number of pieces of core per foot has stabilized to approximately the standard value.

Comparisons Between Shotholes

There were scattered high and low values in the measured properties of the various recovered cores, and no consistant differences were found to indicate azimuth or location dependence. Figures 22 and 23 show some of the damage-analysis results from individual shotholes. Shothole 2 of figure 22 has an unusual number of "tight cores," having permeabilities at or below the standard value of 8-10 μd. The plot showing data from the two remaining holes (SH-1,3) indicates that blasting would increase permeability above the standard level in the small pieces of recovered core within a range of about 25 inches (0.64 m; 6.7 blasthole radii). Figure 23 shows the axial compressive strength and Young's modulus of the core from SH-3 only representing six recovery holes. These plots contain far fewer scattered values than the summary graphs of figures 14 and 15 and clearly show two trends, a strong one out to about 28 inches (0.71 m; 8.6 shothole radii) and a weak one out to about 42 inches (1.07 m; 13 shothole radii), indicating relatively major and minor damage, respectively.

Previous investigators have attributed changes in rock properties to stress unloading rather than explosive damage, and it is possible that some of the observed damage is not blast related. While the Lithonia granite is under great in situ stress, the results of reducing the confining effect of both the overburden and adjacent rock should be the same for both the shothole core and the control hole core. Because the control core data does not exhibit trends attributable to stress effects, it is assumed that blast damage is being observed in the other recovered cores.

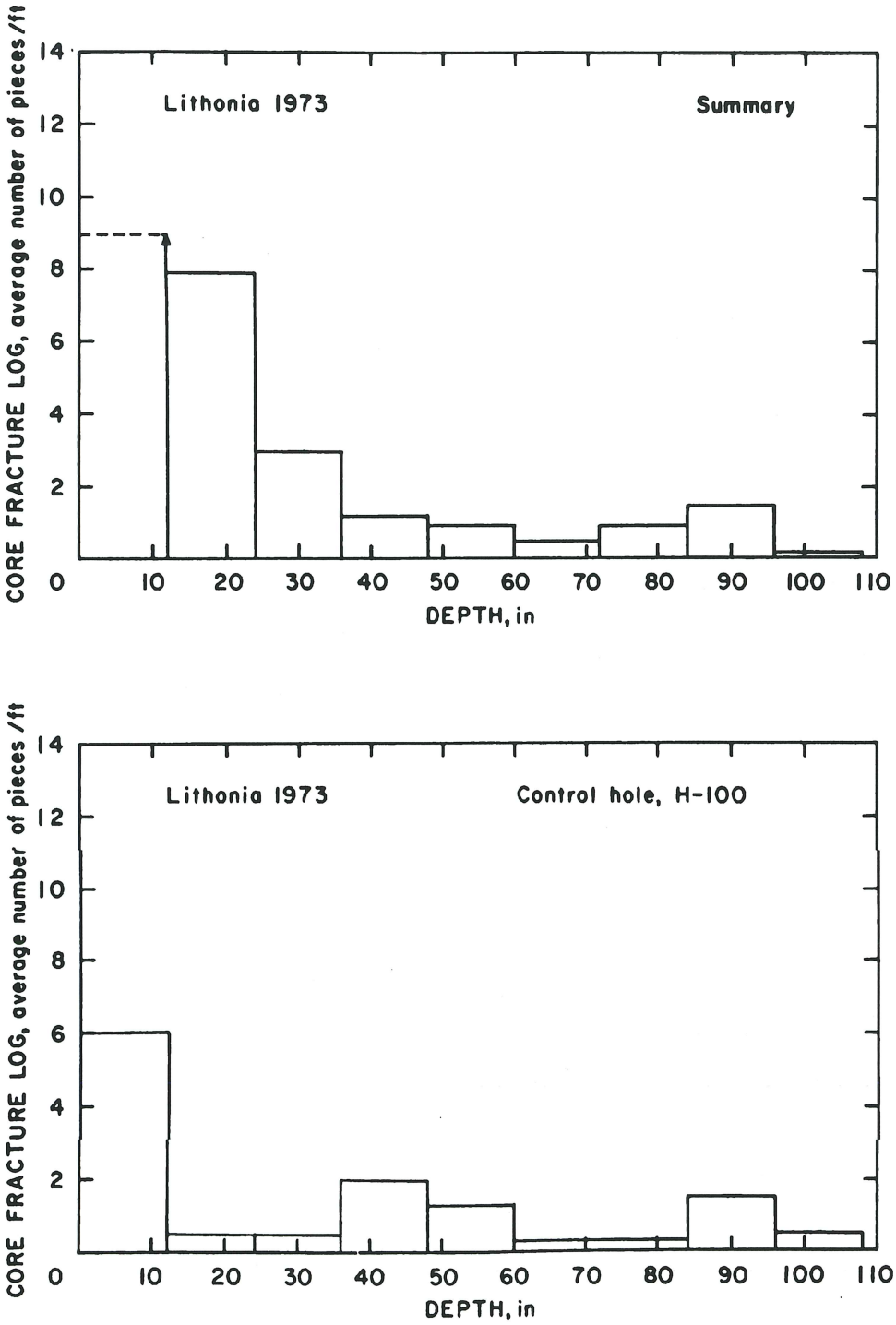

FIGURE 21. - Recovery core analysis, core logs.

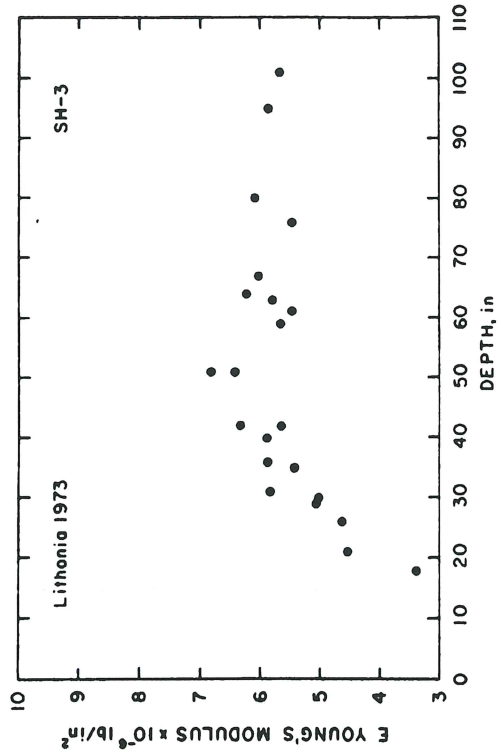

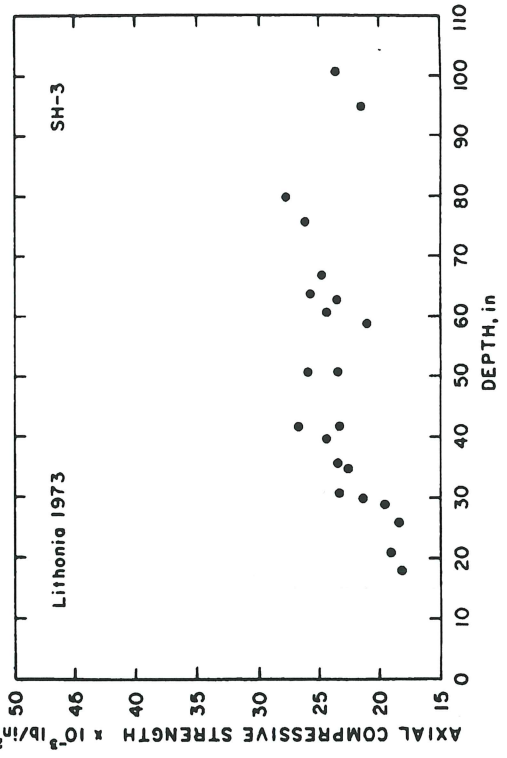

FIGURE 23. - Axial compressive strength and modulus, shothole 3.

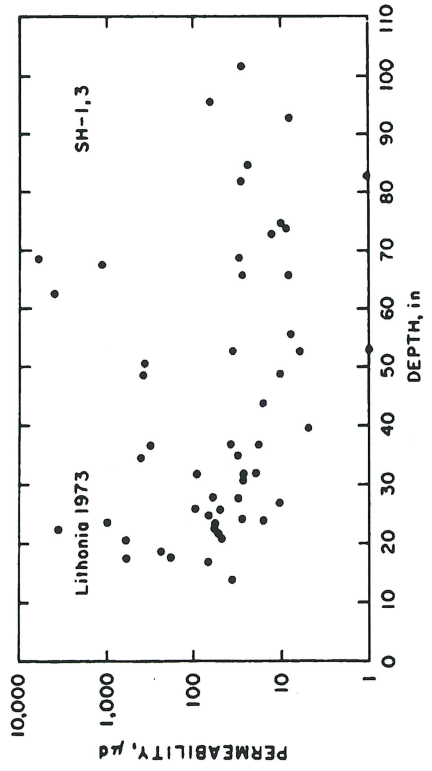

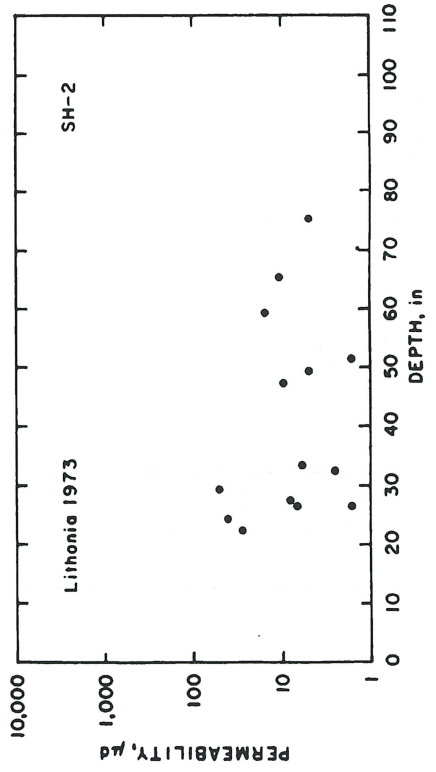

FIGURE 22. - Permeabilities, shotholes 1, 2, and 3.

CONCLUSIONS

The seven fracture state analyses techniques indicate that two zones of blast-produced damage exist in the Lithonia granite from the 6-1/2-in AN-FO loaded production blastholes. All seven techniques (porosity, permeability, Brazilian strength, axial compressive strength, Young's modulus, acoustic sounding, and core fracture logging) indicated that the core is highly damaged out to about 25 inches (0.64 m; 8 blasthole radii). Additionally, the plots of the axial compressive strength, Young's modulus, acoustic results, and recovery core logging suggest that a lesser degree of damage exists between 25 and about 45 inches (1.14 m; 14 blasthole radii). These results suggest that essentially all the core out to approximately 25 inches contains fractures, though not necessarily multi-directional; core between 25 and 45 inches has scattered fracturing; and beyond 45 inches the rock is undamaged. These results in the hard granite-gneiss rock are comparable to previous investigations which found damage out to 18 to 20 charge size radii for a high energy explosive in granite (18); 15 to 22 radii for AN-FO in a relatively soft rock (21); and other values for AN-FO ranging from 20 to 26 radii (7). Table 3 summarizes previous blast fracture work and the present study.

TABLE 3. - Summary of blast-produced damage in rock

Source	Explosive	Rock type	Radius of damage, in charge radii	Crushed zone, in charge radii
Olson (18).....	C-4.....	Granite.....	18-20	-
Siskind (22).....	60 percent dynamite	Shale.....	42-55	-
Do.....	AN-FO.....	.....do.....	15-22	-
Cattermole (6).....	60 percent dynamite	Tuffaceous and pyroclastic.	20-30	3
Colorado School of Mines (7).	-	Soft rock.....	26-29	-
Do.....	-	Hard rock.....	20-23	-
Derlich (9).....	Nuclear (TNT).....	Granite.....	4.9	1.9
Atchison (2).....	-	.....do.....	-	3.0-4.5
D'Andrea (8).....	C-4.....	.....do.....	-	2.3
Siskind (this RI)..	AN-FO.....	.....do.....	14	-

Of all the damage analysis techniques employed, the active acoustic sounding was the most sensitive to fracture detection and has promise for both differentiation between states of fracture and field application. The strength measurements were not as definitive as expected particularly the Brazilian with the biggest problem being the scatter in the data. However, they provided significant fracture-state information when combined with the other techniques. Both the porosity and permeability results provided problems in interpretation. The porosity had anomalous values within the zone of damage, but there were unexplained low values along with the expected high values. Permeability measurements were made on 1-inch long core pieces. Macroscopic permeabilities require the inclusion of the fractures separating the pieces on which the properties are being measured and would be

considerably higher. However, the permeability of these small samples of less than 1 cubic inch gives a better indication of microscopic fracture density and the ability of leaching fluid to permeate the intact rock. Permeability measurements in the field should provide valuable information on the fracture state of a large blast-damaged rock mass for in situ mining.

REFERENCES

1. Atchison, T. C. Fragmentation Principles. Ch. in Surface Mining. AIME, Pfleider, ed., 1968, pp. 355-372.

2. Atchison, T. C., and W. E. Tournay. Comparative Studies of Explosives in Granite. BuMines RI 5509, 1959, 28 pp.

3. Blair, B. E. Physical Properties of Mines Rock. Part III, BuMines RI 5130, 1955, 69 pp.

4. Bur, T. R., R. E. Thill, and K. E. Hjelmstad. An Ultrasonic Method for Determining the Elastic Symmetry of Materials. BuMines RI 7333, 1969, 23 pp.

5. Carroll, R. D., and J. H. Scott. Uphole Seismic Measurements as an Indication of Stress Relief in Granitic Rock Tunnels. U.S. Geol. Survey Prof. Paper 550-D 1966, pp. D138-D143.

6. Cattermole, J. M., and W. R. Hanson. Geologic Effects of the High Explosive Tests in the U.S.G.S. Tunnel Area Nevada Test Site. U.S. Geol. Survey Prof. Paper 382-B, 1962, 29 pp.

7. Colorado School of Mines. Underground Explosion Test Program, ser. I and ser. II experiments, December 1948.

8. D'Andrea, D. V., R. L. Fischer, and A. D. Hendrickson. Crater Scaling in Granite for Small Charges. BuMines RI 7409, 1970, 28 pp.

9. Derlich, S. Underground Nuclear Explosion Effects in Granite Rock Fracturing. Proc. Symp. of Eng. With Nuclear Explosives, Las Vegas, Nev., January 1970, pp. 508-518.

10. Herrmann, L. A. Geology of the Stone Mountain-Lithonia District, Georgia. Dept. of Mines, Mining and Geology, Georgia State Division of Conservation. The Geological Survey Bull. 61, 1954.

11. Hooker, V. E., and W. I. Duvall. Stresses in Rock Outcrops Near Atlanta, Ga. BuMines RI 6860, 1966, 18 pp.

12. Hooker, V. E., and C. F. Johnson. Near-Surface Horizontal Stresses Including the Effects of Rock Anisotropy. BuMines RI 7224, 1969, 29 pp.

13. Kutter, J. K., and C. Fairhurst. On the Fracture Process in Blasting. Int. J. Rock Mech. Min. Sci., v. 8, 1971, pp. 181-202.

14. Miller, J. S., and H. R. Nicholls. Methods and Evaluation of Explosive Fracturing in Oil Shale. BuMines RI 7729, 1973, 22 pp.

15. Nicholls, H. R., and W. I. Duvall. Presplitting Rock in the Presence of a Static Stress Field. BuMines RI 6843, 1966, 19 pp.

16. Nicholls, H. R., and V. E. Hooker. Shear and Longitudinal Waves From HE Detonations in Tuff--Comparison of Tuff and Granite Data. BuMines Applied Physics Res. Lab., Rpt. No. E48.1.1 (final rpt.), 1963, 128 pp; available upon request from Twin Cities Mining Research Center, Minneapolis, Minn.

17. Norman, C. E. Geometric Relationships Between Geologic Structure and Ground Stresses Near Atlanta, Ga. BuMines RI 7365, 1970, 24 pp.

18. Olson, J. J., R. J. Willard, D. E. Fogelson, and K. E. Hjelmstad. Rock Damage From Small Charge Blasting in Granite. BuMines RI 7751, 1973, 44 pp.

19. Scott, J. H., F. T. Lee, R. D. Carroll, and C. S. Robinson. The Construction Parameters in the Straight Creek Tunnel Pilot Bore, Colorado. Int. J. Rock Mech. Min. Sci., v. 5, No. 1, 1968, pp. 1-30.

20. Short, N. M. Progressive Shock Metamorphism of Quartzite Ejecta From the Sedan Nuclear Explosion Crater. J. Geol, v. 78, 1970, pp. 705-732.

21. Siskind, D. E., J. J. Snodgrass, R. A. Dick, and J. N. Quiring. Mine Roof Vibrations From Underground Blasts, Pilot Knob, Mo. BuMines RI 7764, 1973, 21 pp.

22. Siskind, D. E., R. C. Steckley, and J. J. Olson. Fracturing in the Zone Around a Blasthole, White Pine, Mich. BuMines RI 7753, 1973, 20 pp.

23. Ward, M. H. Engineering for In Situ Leaching. Min. Congress J., v. 59, No. 1, January 1973, pp. 21-27.

APPENDIX

TABLE A-1. Porosity and permeability measurements

Blasthole (SH)	Recovery hole (H)	Distance from center of blasthole		Porosity, percent	Permeability, µd	Laboratory test identification
		Inches	m			
1	1	10	0.25	3.8	-	1
1	1	10.8	.27	.8	-	2
1	1	11.8	.30	4.5	-	3
1	1	12.5	.32	3.6	-	4
1	1	16.5	.42	-	36.3	4728
1	1	19	.48	-	226	4729
1	1	20.5	.52	2.8	-	5
1	1	21.3	.54	3.0	-	6
1	1	23	.58	-	57.2	4730
1	1	24.5	.62	2.9	26.8	4731
1	1	33.3	.84	.6	-	7
1	1	34	.86	2.1	-	8
1	1	32	.81	-	89.2	4732
1	1	35	.89	2.9	32.1	4733
1	1	45.8	1.17	2.7	-	9
1	1	49	1.30	2.9	373	4734
1	1	67	1.70	3.0	42,700	4735
1	1	69	1.75	-	5,500	4736
1	1	83	2.11	2.9	<1	4737
1	1	96	2.44	-	59.5	4738
1	2	18	.46	3.7	616	4739
1	2	18.3	.47	3.5	-	10
1	2	20.5	.52	-	44.5	4740
1	2	21	.53	2.0	-	11
1	2	23	.58	3.1	3,490	4741
1	2	25	.64	2.8	66.1	4742
1	2	27.8	.70	2.7	-	12
1	2	35	.89	-	403	4743
1	2	37	.94	2.4	301	4744
1	2	56	1.42	2.2	7.66	4745
1	2	68	1.73	-	1,160	4746
1	3	16	.41	2.5	-	13
1	3	17	.43	4.0	-	14
1	3	18	.46	2.6	178	4747
1	3	20	.51	4.0	-	15
1	3	22	.56	-	53.3	4748
1	3	28	.71	2.4	30.7	4749
1	3	53	1.35	2.6	32.8	4750
1	3	63	1.62	2.9	-	16
1	3	66	1.67	-	7.72	4751
1	3	85	2.16	2.5	22.0	4752
2	1	15	.38	3.2	-	17
2	1	19	.48	1.2	-	18

TABLE A-1. - Porosity and permeability measurements--Continued

Blasthole (SH)	Recovery hole (H)	Distance from center of blasthole		Porosity, percent	Permeability, μd	Laboratory test identification
		Inches	m			
2	1	20	.51	3.2	-	19
2	1	22	.56	2.6	25.2	4753
2	1	29	.74	2.7	-	20
2	1	33	.84	-	5.56	4754
2	1	49	1.24	-	4.68	4755
2	1	75	1.90	2.5	4.67	4756
2	2	15	.38	3.0	-	21
2	2	16	.41	2.2	-	22
2	2	17	.43	3.5	-	23
2	2	26	.66	2.6	1.50	4757
2	2	32	.81	2.6	2.35	4758
2	2	51	1.30	-	1.50	4759
2	3	19	.48	-	50.7	4762
2	3	21	.53	1.1	-	24
2	3	23	.58	4.3	-	25
2	3	26	.66	2.7	6.42	4760
2	3	59	1.50	3.0	14.3	4761
2	4	13	.33	.7	-	26
2	4	23	.58	3.5	-	27
2	4	24	.61	3.0	41.7	4763
2	4	27	.69	2.6	7.88	4764
2	4	47	1.19	2.0	9.42	4765
2	4	65	1.65	-	10.9	4766
3	1	14	.36	4.1	-	28
3	1	17	.43	.8	-	29
3	1	24	.61	2.6	14.2	4767
3	1	22	.56	.2	-	30
3	1	27	.69	2.7	11.0	4768
3	1	37	.94	-	17.5	4769
3	1	44	1.12	3.4	14.3	4770
3	1	50	1.29	-	343	4771
3	1	51	1.31	3.4	-	31
3	1	73	1.85	-	12.4	4772
3	1	93	2.36	-	7.92	4773
3	2	17	.43	5.8	-	32
3	2	21	.53	1.2	0	33
3	2	31	.79	3.0	25.4	4774
3	2	53	1.35	3.0	<1	4775
3	2	75	1.90	-	9.50	4776
3	2	103	2.62	-	26.6	4777
3	3	21	.53	-	601	4778
3	3	23	.58	1.8	-	34
3	3	24	.61	3.3	955	4779
3	3	26	.66	3.3	93.8	4780
3	3	32	.81	2.4	25.0	4781

TABLE A-1. Porosity and permeability measurements--Continued

Blasthole (SH)	Recovery hole (H)	Distance from center of blasthole		Porosity, percent	Permeability, μd	Laboratory test identification
		Inches	m			
3	3	66	1.68	-	27.6	4782
3	4	16	.41	4.3	-	35
3	4	17	.43	3.1	67.4	4783
3	4	18	.46	2.1	-	36
3	4	23	.58	3.2	56.1	4784
3	4	32	.81	2.8	19.0	4785
3	4	63	1.60	2.8	3,890	4786
3	4	82	2.08	-	25.1	4787
3	5	26	.66	-	48.8	4788
3	5	40	1.02	2.7	4.82	4789
3	5	53	1.35	-	6.24	4790
3	5	69	1.75	2.9	28.0	4791
3	6	28	.71	3.3	61.9	4792
3	6	30	.76	3.3	-	37
3	6	37	.94	3.0	36.4	4793
3	6	49	1.24	2.6	11.0	4794
3	6	74	1.88	-	8.8	4795
-	100	1.5	.04	2.3	14.0	4796
-	100	3	.08	2.1	17.3	4797
-	100	10.5	.27	2.1	9.49	4798
-	100	22	.56	-	3.23	4799
-	100	29.5	.75	-	6.15	4800
-	100	40.5	1.03	-	9.31	4801
-	100	53	1.35	-	5.46	4802
-	100	71	1.80	-	1.56	4803
-	100	85.5	2.17	-	4.67	4804
-	100	92	2.34	2.4	4.67	4805
-	100	111.5	2.83	-	4.70	4806
-	100	117	2.98	3.3	-	38

TABLE A-2. Compressive strength and Young's modulus

Blasthole (SH)	Recovery hole (H)	Distance from center of blasthole		Uniaxial compressive strength		Young's modulus		Laboratory test identification
		Inches	m	10^3 lb/in^2	10^6 N/m^2	10^6 lb/in^2	10^9 N/m^2	
1	1	16.3	0.42	18.2	125	4.56	31.4	4807
1	1	40	1.02	35.5	245	9.90	68.3	4808
1	1	51	1.30	32.9	226	9.62	66.4	4809
1	1	75	1.90	25.9	178	8.42	58.1	4810
1	1	106	2.69	31.7	219	9.63	66.4	4811
1	2	32	.81	22.2	153	6.94	47.9	4812
1	2	51	1.30	26	179	8.38	57.8	4813
1	3	24	.61	37.8	261	7.33	50.5	4815
1	3	37	.94	26.8	184	8.21	56.6	4816
1	3	55	1.40	23.6	162	6.72	46.3	4817
1	3	79	2.00	24.5	169	6.05	41.7	4818
2	1	35	.89	29.5	203	6.53	45.0	4819
2	1	51	1.30	23.4	161	5.79	39.9	4820
2	1	77	1.95	25.8	178	5.99	41.3	4821
2	2	30	.76	22.9	158	5.71	39.4	4822
2	2	59	1.50	22.4	154	5.74	39.6	4823
2	3	28	.71	23.5	162	5.19	35.8	4824
2	3	61	1.55	22.0	152	5.63	38.8	4825
2	4	29	.74	20.2	139	4.62	31.8	4826
2	4	49	1.24	20.7	143	5.15	35.5	4827
3	1	19	.48	-	-	-	-	4828
3	1	31	.79	23.3	161	5.87	40.5	4829
3	1	42	1.07	26.8	185	6.38	44.0	4830
3	1	59	1.50	21.2	146	5.69	39.2	4831
3	1	95	2.41	21.7	149	5.93	40.9	4832
3	2	26	.66	18.3	126	4.65	32.0	4833
3	2	42	1.07	23.3	161	5.69	39.2	4834
3	2	63	1.60	23.7	164	5.84	40.2	4835
3	2	101	2.56	23.8	164	5.77	39.8	4836
3	3	30	.76	21.3	147	5.05	34.8	4837
3	3	64	1.62	25.8	178	6.29	43.4	4838
3	4	21	.53	19.0	131	4.54	31.3	4839
3	4	36	.91	23.5	162	5.90	40.6	4840
3	4	61	1.55	24.5	169	5.52	38.1	4841
3	4	80	2.03	27.8	192	6.16	42.5	4842
3	5	18	.46	17.7	122	3.41	23.5	4843
3	5	29	.74	19.6	135	5.08	35.0	4844
3	5	51	1.30	23.5	162	6.87	47.4	4845
3	5	67	1.70	24.8	171	6.10	42.1	4846
3	6	35	.89	22.7	157	5.47	37.7	4847
3	6	40	1.02	24.5	169	5.92	40.8	4848
3	6	51	1.30	26.1	180	6.48	44.6	4849
3	6	76	1.93	26.3	181	5.51	38.0	4850
-	100	6	.15	30.8	212	6.57	45.3	4851
-	100	20	.51	27.2	188	6.61	45.6	4852
-	100	42.5	1.08	27.6	190	6.36	43.9	4853
-	100	55	1.40	29.0	200	6.65	45.8	4854
-	100	82.5	2.09	28.5	196	6.49	44.7	4855
-	100	113.5	2.88	26.2	181	6.15	42.4	4856

TABLE A-3. - Acoustic measurements and Brazilian strength

Blasthole (SH)	Recovery hole (H)	Travel time, μsec				Brazilian strength		Laboratory test identification
		0°	45°	90°	135°	lb/in	10^8 N/m	
1	1	11.75	12.15	11.95	11.65	680	0.118	4728
1	1	13.15	12.95	13.45	12.65	630	.111	4729
1	1	11.75	11.55	11.25	11.65	1,060	.185	4730
1	1	11.95	12.15	12 75	12.65	680	.118	4731
1	1	11.75	12.45	11.65	11.05	700	.122	4732
1	1	11.45	10.75	11.15	11.65	670	.117	4733
1	1	9.25	8.05	8.45	9.25	950	.167	4734
1	1	8.95	10.25	9.85	8.25	460	.081	4735
1	1	9.45	10.80	9.05	7.95	650	.115	4736
1	1	9.05	8.35	9.45	10.05	1,590	.278	4737
1	1	9.85	8.65	9.35	11.15	1,360	.238	4738
1	2	14.65	13.35	13.95	16.35	430	.076	4739
1	2	11.85	10.85	12.55	13.75	720	.126	4740
1	2	13.65	11.85	11.95	13.85	730	.128	4741
1	2	12.75	14.00	13.15	11.55	1,220	.214	4742
1	2	11.15	10.75	10.35	10.75	1,020	.178	4743
1	2	10.45	9.95	10.75	10.25	1,040	.181	4744
1	2	9.25	8.85	9.75	10.35	1,230	.215	4745
1	2	8.75	8.75	9.85	8.85	1,180	.207	4746
1	3	13.35	15.5	14.25	12.45	470	.083	4747
1	3	12.85	12.35	13.15	14.15	910	.160	4748
1	3	11.85	12.75	12.95	11.65	970	.170	4749
1	3	9.05	7.95	8.85	9.40	1,010	.177	4750
1	3	9.35	9.85	8.85	8.65	910	.159	4751
1	3	9.45	10.55	10.95	9.55	1,680	.294	4752
2	1	12.45	13.55	11.95	12.05	860	.151	4753
2	1	10.55	9.25	9.65	11.25	1,000	.176	4754
2	1	9.45	8.75	9.55	10.35	1,400	.244	4755
2	1	10.45	9.05	8.85	10.05	1,530	.267	4756
2	2	9.75	9.45	11.05	11.25	1,480	.259	4757
2	2	9.75	9.05	11.00	11.15	1,440	.252	4758
2	2	8.55	9.65	10.45	9.65	1,290	.226	4759
2	3	11.15	10.05	9.15	9.35	1,600	.280	4760
2	3	11.45	10.25	9.25	10.35	1,000	.175	4761
2	3	12.95	13.45	14.65	14.80	620	.108	4762
2	4	12.15	10.85	12.05	13.15	1,220	.214	4763
2	4	11.45	11.15	11.65	11.85	1,480	.259	4764
2	4	10.05	9.15	10.15	11.25	1,380	.242	4765
2	4	9.55	9.45	10.65	10.45	1,040	.183	4766
3	1	9.75	10.55	11.05	9.85	880	.155	4767
3	1	8.85	9.55	10.95	9.35	730	.128	4768
3	1	11.75	11.55	10.65	10.75	1,630	.285	4769
3	1	12.05	11.45	9.95	11.05	830	.146	4770
3	1	11.05	9.05	9.95	11.65	1,000	.176	4771
3	1	9.35	8.75	9.45	10.65	1,410	.247	4772
3	1	7.75	8.05	9.55	9.75	830	.146	4773
3	2	11.65	11.15	12.15	12.45	580	.101	4774

TABLE A-3. - Acoustic measurements and Brazilian strength--Continued

Blasthole (SH)	Recovery hole (H)	Travel time, μsec				Brazilian strength		Laboratory test identification
		0°	45°	90°	135°	lb/in	10^6 N/m	
3	2	9.95	8.85	7.95	9.15	1,400	0.245	4775
3	2	8.65	10.05	10.65	8.65	1,330	.234	4776
3	2	10.35	10.35	11.75	11.25	790	.138	4777
3	3	14.05	14.65	13.55	13.75	160	.028	4778
3	3	12.95	13.35	13.85	13.65	610	.107	4779
3	3	13.15	13.35	12.65	12.95	670	.117	4780
3	3	12.45	11.95	11.45	12.15	830	.145	4781
3	3	8.85	8.95	9.65	10.45	1,780	.311	4782
3	4	11.65	11.35	12.20	11.05	470	.083	4783
3	4	11.85	12.35	13.05	11.95	700	.123	4784
3	4	11.65	11.05	11.35	11.95	950	.131	4785
3	4	9.45	11.55	11.45	9.45	940	.148	4786
3	4	9.00	9.15	10.55	10.80	740	.129	4787
3	5	11.25	10.75	11.85	11.65	650	.113	4788
3	5	11.05	9.95	10.05	11.25	1,100	.193	4789
3	5	9.45	9.45	10.65	10.75	960	.167	4790
3	5	9.65	11.05	11.15	9.75	1,310	.230	4791
3	6	12.55	12.45	12.05	12.50	570	.100	4792
3	6	11.35	11.95	12.65	11.60	950	.166	4793
3	6	9.55	10.35	11.15	10.05	1,640	.287	4794
3	6	8.95	9.65	10.95	10.25	1,180	.207	4795
-	100	11.45	9.85	8.15	9.95	1,420	.249	4796
-	100	11.55	10.35	8.65	9.75	1,500	.263	4797
-	100	10.55	8.85	9.35	11.25	1,650	.288	4798
-	100	8.55	7.65	8.75	9.35	1,690	.296	4799
-	100	8.45	9.35	10.75	9.75	1,070	.188	4800
-	100	8.65	8.95	10.85	10.25	1,000	.174	4801
-	100	8.15	9.90	9.45	8.25	1,350	.237	4802
-	100	9.95	10.75	9.35	8.15	810	.141	4803
-	100	9.95	9.55	8.35	8.65	1,520	.267	4804
-	100	10.25	10.05	8.65	8.85	900	.158	4805
-	100	10.75	9.35	8.15	9.25	1,050	.185	4806

TABLE A-4. - Core log data

Depth, feet	Number of pieces of recovered core													
	Shothole 1			Shothole 2				Shothole 3						
	H-1	H-2	H-3	H-1	H-2	H-3	H-4	H-1	H-2	H-3	H-4	H-5	H-6	H-100
1	8-1/3+	-	-	-	-	-	-	-	-	-	-	-	-	6
2	9	9	6	6	5	6	13	10	7	-	7	7	9	1/2
3	5-1/2	4	3	3	1/4	1/4	1/4	3	1	3-1/4	3	1	4	1/2
4	2	1	1	1/4	1/4	1/4	1/4	2	5	1/4	2	1-1/2	1-1/4	2
5	2	1/2	1-1/2	1/4	1/4	1/4	1/4	2	1	1/4	3-1/2	1/2	1/3	1-1/3
6	1	1/2	1/2	1/4	1/4	3/4	1/2	1/4	1/4	1/4	3/4	1/2	1/3	1/3
7	1/4		1	1				1/4	1/4	2	1/2		2-1/2	1/3
8	1/4		2					1/4	1/4		5-1/4			1-1/2
9	1/4							1/4	1/4					1/2

INT.-BU.OF MINES,PGH.,PA. 19286

*U.S. GOVERNMENT PRINTING OFFICE: 1974-708-740/816